

# Journal Pre-proof

New insights on Lower Ordovician (Floian) reefs from the Argentine Precordillera: Biostratigraphic, sedimentologic and paleogeographic implications

Ana Mestre, Susana Heredia, Florencia Moreno, Leandro Benegas, Andres Morfil, Tatiana Soria



PII: S0895-9811(20)30344-8

DOI: <https://doi.org/10.1016/j.jsames.2020.102801>

Reference: SAMES 102801

To appear in: *Journal of South American Earth Sciences*

Received Date: 19 May 2020

Revised Date: 31 July 2020

Accepted Date: 31 July 2020

Please cite this article as: Mestre, A., Heredia, S., Moreno, F., Benegas, L., Morfil, A., Soria, T., New insights on Lower Ordovician (Floian) reefs from the Argentine Precordillera: Biostratigraphic, sedimentologic and paleogeographic implications, *Journal of South American Earth Sciences* (2020), doi: <https://doi.org/10.1016/j.jsames.2020.102801>.

This is a PDF file of an article that has undergone enhancements after acceptance, such as the addition of a cover page and metadata, and formatting for readability, but it is not yet the definitive version of record. This version will undergo additional copyediting, typesetting and review before it is published in its final form, but we are providing this version to give early visibility of the article. Please note that, during the production process, errors may be discovered which could affect the content, and all legal disclaimers that apply to the journal pertain.

© 2020 Published by Elsevier Ltd.

**Author Statement**

**“New insights on Lower Ordovician (Floian) reefs from the Argentine Precordillera: biostratigraphic, sedimentologic and paleogeographic implications”**

by Mestre, Ana, Heredia, Susana, Moreno, Florencia, Benegas, Leandro, Morfil, Andres and Soria, Tatiana.

Dear editor:

A detailed description of the diverse contributions to the work is shown.

Dr. Ana Mestre: Conceptualization, methodology, conodont and microfacies analysis, writing - review and editing. Supervision. Funding acquisition and project administration.

Dr. Susana Heredia: Conceptualization, methodology, conodont analysis, writing - review and supervision.

Lic. Moreno, Florencia: Conceptualization, methodology, conodont and microfacies analysis, writing - review and editing.

Lic. Leandro Benegas: Methodology, conodont and microfacies analysis, Figure editing.

Lic. Andres Morfil: Methodology, conodont and microfacies analysis, Figure editing.

Dr. Soria, Tatiana: Methodology, conodont and microfacies analysis.

1 **New insights on Lower Ordovician (Floian) reefs from the Argentine**  
2 **Precordillera: biostratigraphic, sedimentologic and paleogeographic implications**

3

4 Mestre, Ana<sup>1</sup>, Heredia, Susana<sup>1</sup>, Moreno, Florencia<sup>1</sup>, Benegas, Leandro<sup>2</sup>, Morfil,  
5 Andres<sup>2</sup> and Soria, Tatiana<sup>3</sup>

6

7 1 CONICET-CIGEOBIO-Lab. de Micropaleontología-IIM-Facultad de Ingeniería,  
8 Universidad Nacional de San Juan, Av. Libertador General San Martín 1109 (O).  
9 [amestre@unsj.edu.ar](mailto:amestre@unsj.edu.ar); [sheredia@unsj.edu.ar](mailto:sheredia@unsj.edu.ar); [fbmoreno@unsj.edu.ar](mailto:fbmoreno@unsj.edu.ar)

10 2 Departamento de Geología-Facultad de Ciencias Exactas, Física y Naturales, Av.  
11 Ignacio de la Roza y Meglioli. [leandrobeneegas.geo@gmail.com](mailto:leandrobeneegas.geo@gmail.com), [morfil\\_23@hotmail.com](mailto:morfil_23@hotmail.com)

12 3 CONICET-Instituto y Museo de Ciencias Naturales. Universidad Nacional de San  
13 Juan-CIGEOBIO. [tsoria@unsj.edu.ar](mailto:tsoria@unsj.edu.ar)

14 **Corresponding Author:** Ana Mestre, [amestre@unsj.edu.ar](mailto:amestre@unsj.edu.ar)

15

16

17

18

19

20

21 **Abstract**

22 The shallow carbonate facies of the middle part from the San Juan Formation that  
23 outcrops in the Central Precordillera is studied in the present contribution in order to  
24 assess conodont biostratigraphy and sedimentology. Three facies and five microfacies  
25 were recognized in the Niquivil and Talacasto sections. These facies represent three  
26 genetically-related depositional facies from distal to proximal, and include from shallow  
27 subtidal facies below wave action to shoal and reef facies. This reef and shoal facies is  
28 recorded for the first time at the Talacasto section. The reef framework consists mainly  
29 of calcimicrobes in consortia with pulchrilaminids, calathids and lithistid sponges  
30 conforming a microbial-metazoan matrix-supported reef. The pulchrilaminid  
31 *Zondarella communis* Keller and Flügel, present in these reef facies, is here assigned for  
32 first time to the late Floian (Early Ordovician), *Oepikodus intermedius* conodont Zone.  
33 In this sense, the Precordilleran reefs represent the latest Floian record of  
34 pulchrilaminids compared to the worldwide records for these Early Ordovician reef-  
35 builder organisms. This provides crucial information for understanding the dispersal  
36 pathways of these organisms, and allows a paleogeographic reconstruction of the  
37 western margin of Gondwana in the Early Ordovician.

38

39

40

41

42

43

## 44 1. Introduction

45 During the Early-Middle Ordovician, the Precordillera (NW Argentina) was  
46 mainly occupied by an extensive shallow-water mixed platform, on which a carbonate  
47 system was developed in the central part of the basin, in the current province of San  
48 Juan.

49 The San Juan Formation is a Lower-Middle Ordovician classic unit from the  
50 Precordillera. It was redefined by Keller *et al.* (1994) as composed by limestone and  
51 marly limestone with rich open marine fossils at La Silla section (Central Precordillera)  
52 (Beresi, 1986; Herrera and Benedetto, 1991; Beresi and Rigby, 1993; Vaccari 1994;  
53 Sánchez *et al.*, 1996; Carrera, 1997). Different carbonate and mixed carbonate facies in  
54 the San Juan Formation were recognized by Cañas (1999), Keller (1999), Mestre (2014)  
55 and Soria *et al.* (2017), among others. The Ordovician reef shallow facies from this  
56 classic unit was studied by several authors (Cañas and Keller, 1993; Keller and  
57 Bordonaro, 1993; Carrera and Cañas, 1997; Cañas and Carrera, 2003) who provided  
58 different information about reef facies, which are mainly composed by microbial,  
59 lithistid sponges, calathids and *Zondarella communis* Keller and Flügel, 1996  
60 (pulchrilaminids by Stearn *et al.*, 1999).

61 Reefs are defined as calcareous deposits created by essentially in-place sessile  
62 organisms (Riding, 2002). The skeletal reef ecosystems became dominant in the latest  
63 Middle–Late Ordovician in the world. In contrast, Early Ordovician reefs were  
64 dominated by microbial components, together with calathids and lithistid sponges  
65 (Church, 1974; Toomey and Nitecki, 1979; Pratt and James, 1989; Cañas and Carrera,  
66 1993, Li *et al.*, 2015). The earliest occurrence of pulchrilaminids in the Early  
67 Ordovician reefs was documented in South China, and then in Laurentia (Toomey and  
68 Nitecki, 1979; Pratt and James, 1982; Adachi *et al.*, 2011, 2012). Furthermore, Keller

69 and Flügel (1996) described the genus *Zondarella* (included later in the Order  
70 Pulchrilaminida by Webby, 2012) which was involved in the upper reef horizon from  
71 the Argentine Precordillera. This reef horizon would have developed during the  
72 Dapingian times (early Middle Ordovician) (Lehnert and Keller, 1993; Keller and  
73 Flügel, 1996, Albanesi et al., 2003; Cañas and Carrera, 2003).

74 In the Central Precordillera, the distribution of the upper reef horizon that  
75 includes the reef-builder *Zondarella communis* is restricted to the north part of this  
76 region (Cañas and Carrera, 2003), and its presence southward still remains unknown.  
77 For this reason, the exploration of the new areas and sections in the Central  
78 Precordillera where this reef facies is present is an imperative assignment for increasing  
79 the knowledge on the distribution and paleoenvironment analysis of this important  
80 facies in the Ordovician Precordillera basin.

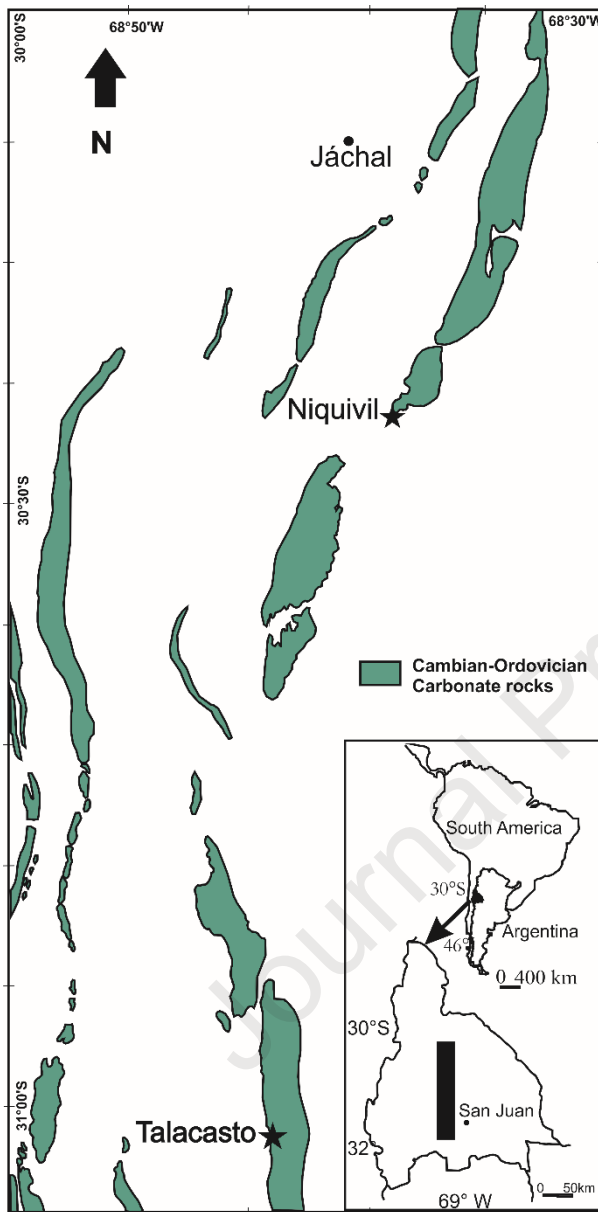
81 The *Tripodus laevis/Baltoniodus triangularis* Zone (early Dapingian) was  
82 recorded through the upper strata of the San Juan Formation which overlies the upper  
83 reef horizon in the Niquivil section (Mango and Albanesi, 2018a), contrary to a  
84 previous record that assumed the upper reef horizon as correlative with the *T. laevis* and  
85 *B. navis* zones (Dapingian) in the same section (Albanesi et al., 2003; 2006). This  
86 controversy led to restudy the conodont biostratigraphy of this reef horizon.

87 The aim of this contribution is to carry out biostratigraphic and sedimentologic  
88 studies on the middle part of the San Juan Formation in the Niquivil (31°00'30,87''S –  
89 68°46'11,80W) and Talacasto (30°24'20,63''S – 68°41'07,70''W) sections (Fig. 1) at  
90 the Central Precordillera where the reef and shoal facies are developed, in order to  
91 provide an assessment of biostratigraphic and paleogeographic significance of these  
92 facies in a regional and global context.

93

94

95



96

97 **Figure 1:** Location map of the study sections from the Central Precordillera. The black  
 98 stars indicated the Niquivil and Talacasto sections.

99

## 100 2. Geological setting

101 The Precordillera is located in western Argentina and extends through the  
 102 provinces of La Rioja, San Juan, and Mendoza, where Cambrian-Ordovician carbonate

103 and siliciclastic successions are developed in a shelf environment. The San Juan  
104 Formation represents the youngest carbonate unit that is followed by a transitional  
105 diachronous succession that consists of nodular marlstones, parted limestones  
106 interbedded with black shale, or only black shale through the Lower to Middle  
107 Ordovician (Baldis et al., 1982; Keller, 1999; Astini, 2003; Mestre and Heredia, 2013;  
108 Mestre, 2014). The oldest conodonts recovered from the San Juan Formation  
109 demonstrate a late Tremadocian age for the base of this unit, recording the *Paltodus*  
110 *deltifer* Zone (Keller et al., 1994; Albanesi et al., 1998). The top of the San Juan  
111 Formation has been dated at several localities. In the northern and south sections,  
112 conodonts rendered a Lower Ordovician age (*Oepikodus intermedius* Zone) for the  
113 transitional beds between the San Juan Formation and the black shale of the overlying  
114 Gualcamayo Formation (Heredia et al., 2009; Soria, 2017), whereas elsewhere in central  
115 sections, conodonts have proved a Darriwilian age for the upper limestone beds of the  
116 San Juan Formation (Lehnert, 1995; Albanesi et al., 1998; Heredia and Mestre, 2011;  
117 2013; Mestre, 2012; 2014; Heredia et al., 2017).

118         The reef facies were first mentioned in the Precordillera by Baldis et al. (1981)  
119 in the Upper Cambrian La Flecha Formation. After that, the Upper Cambrian  
120 thrombolithic microbialites were recorded in the La Silla Formation (Keller, 1999;  
121 Cañas, 2002). The most recent study in the La Silla Formation describes a reef mound,  
122 where the *Amsassia argentina* Carrera *et al.* (coral-like organism) constitutes the main  
123 framework builder organism together with a complex microbial consortium, and these  
124 organisms belongs to the latest Cambrian–Early Ordovician (Carrera et al., 2017).

125         In the San Juan Formation, diverse organic buildups have been recorded  
126 including the microbialites-sponge reefs and “stromatoporoid”-sponges-receptaculite  
127 reefs in the lower and upper part of this unit (Cañas and Carrera, 1993; Cañas and



128 Keller, 1993; Keller and Bordonaro, 1993; Carrera and Cañas, 1996; Keller and Flügel,  
129 1996), as well as in the “Ponón Trehué” Formation (Lehnert et al., 1998) at the  
130 southernmost of Cuyania.

131 Cañas and Carrera (2003) presented a summary of the Ordovician Precordilleran  
132 reefs, describing two Tremadocian reef types and two Middle Ordovician reef types.  
133 The Middle Ordovician reefs are composed by the Microbialite-*Zondarella-Calathium*  
134 reefs, present in the middle part of the San Juan Formation at the Central Precordillera,  
135 and the *Zondarella*-dominated reefs, present in the upper part of the San Juan Formation  
136 at the Eastern Precordillera. However, both were included in upper reef horizon (Keller,  
137 1999; Lehnert and Keller, 1993; Cañas and Carrera, 2003).

138 Based on the conodont assemblages recovered from the Microbialite-  
139 *Zondarella-Calathium* reefs and *Zondarella*-dominated reefs in Central and Eastern  
140 Precordillera accordingly, Lehnert and Keller (1993) constrained these levels from the  
141 *Baltoniodus navis* to “*Amorphognathus*” *variabilis* zones (Middle Ordovician).  
142 However, in the Río Sasso section, these authors recorded the oldest conodont  
143 association with isolated *Zondarella* sp., indicating the *Oepikodus intermedius* –  
144 *Baltoniodus triangularis* zones for these levels. Also, Lehnert et al. (1998) proposed the  
145 *Oepikodus intermedius* Zone for the upper biostromal complex present in the “Ponón  
146 Trehué” Formation. On the other hand, Albanesi et al. (2006) proposed the *Tripodus*  
147 *laevis* and *Baltoniodus navis* conodont zones (Dapingian) for the Microbialite-  
148 *Zondarella-Calathium* reefs.

149

### 150 3. Methods

151 This study is based on detailed field observations and laboratory analyses of thin  
152 and polished sections. The Niquivil and Talacasto sections were logged for the

153 construction of lithological columns of the shoal and reef facies from the San Juan  
154 Formation (Fig. 2). Also, twenty-two rock samples were collected from these facies. In  
155 the Micropaleontology Laboratory, forty thin and polished sections were made in order  
156 to identify fossils and analyze the distribution of shoal components. A petrological  
157 investigation of the thin and polished sections was performed using Leica DM2700  
158 microscopes and Lanset binocular microscopes.

159 Fifteen conodont samples were collected from shoal and reef facies in the  
160 Talacasto section on the same levels sampled by Soria et al. (2013), and five samples  
161 were productive for conodonts. Also, eleven beds previously studied by Albanesi et al.  
162 (2003, 2006) were resampled (Fig. 2, Table 1). From these, only 6 samples were  
163 productive for conodonts. Initially, 1–2 kg of each sample was dissolved in diluted  
164 formic acid with additional material processed if needed, following the Stone (1987)  
165 methods. The insoluble fraction of each sample was picked for conodonts resulting in  
166 recovery of *ca.* 200 identifiable and fragmented conodont elements. Conodonts are  
167 housed in the collection of the INGEO at the Universidad Nacional de San Juan, under  
168 the code-MP.

169

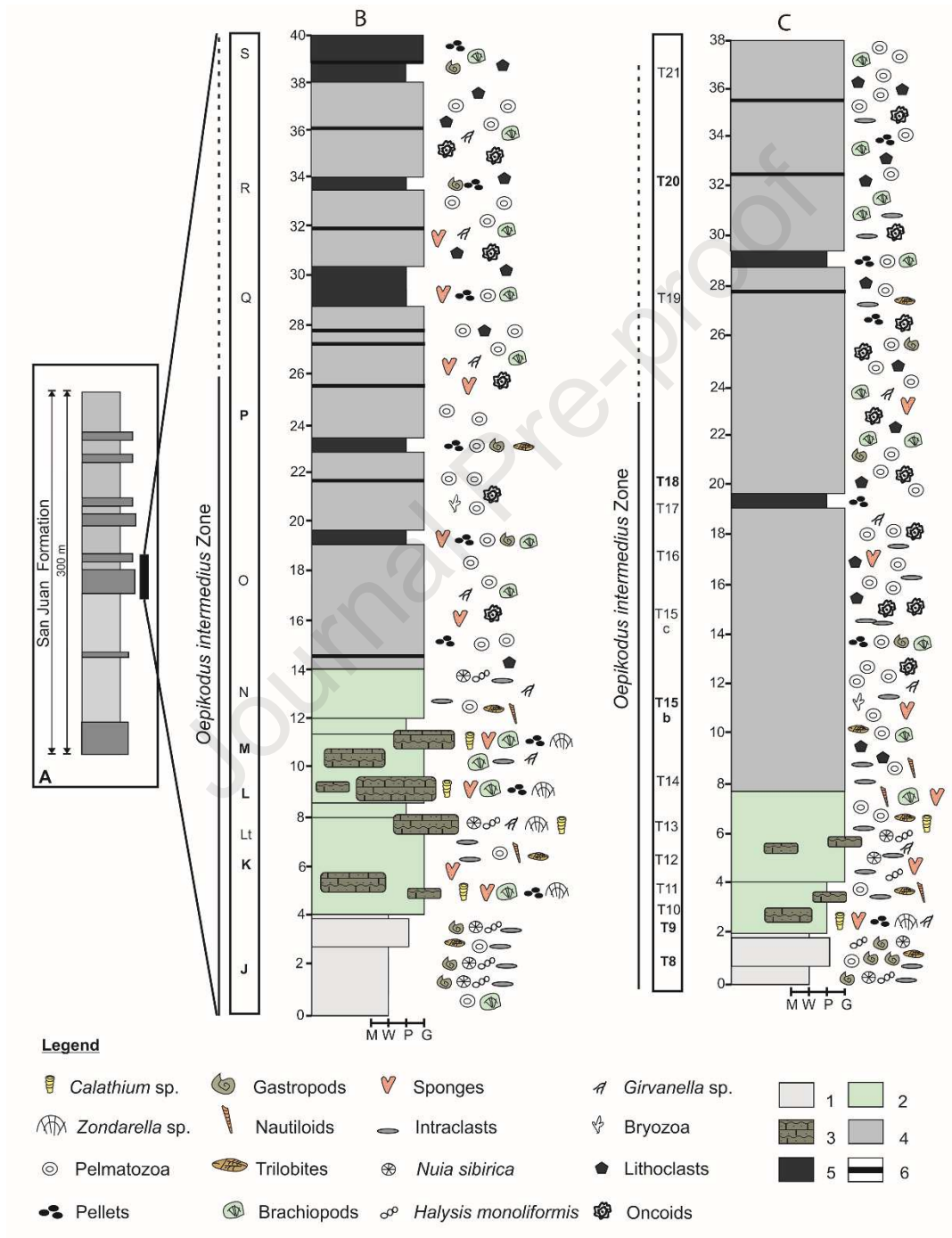
#### 170 **4. Conodont biostratigraphy**

171 In order to date the shoal and reef facies recognized in the Talacasto and  
172 Niquivil sections (Figs. 1, 2, Table 1), samples from these levels were examined for  
173 their conodont content. The conodont assemblages recovered from samples belong to  
174 the *O. intermedius* Zone, late Floian (Early Ordovician). The zonal key conodont *O.*  
175 *intermedius* Serpagli, is accompanied by the more abundant species  
176 *Bergstroemognathus extensus* Serpagli, *Juanognathus variabilis* Serpagli, few  
177 specimens of *Cooperignathus aranda* (Cooper), and the typical Gondwanan conodont

178 species *Erraticodon patu* Cooper (Heredia et al., 2013), as well as a few more long-  
 179 ranging taxa (Fig. 3).

180

181



182

183 **Figure 2:** Stratigraphy column of the shoal and reef facies from Niquivil (B) and  
 184 Talacasto sections (C) (vertical scale in meters). The samples in bold font are the

185 productive conodont samples. A- Schematic stratigraphic column of the San Juan  
186 Formation. The microfacies are represented by 1- Nodular biointraclastic wackestone-  
187 packstone, 2- Biointraclastic packstone-grainstone, 3- Microbial-Skeletal boundstone,  
188 4- Intrabioclastic grainstone, 5- Peloidal packstone-grainstone, 6- Chert.

189

190 The *Oepikodus intermedius* Zone has already been recorded in several sections  
191 in the San Juan Formation by Sarmiento (1990), Lehnert (1993, 1995), Albanesi et al.  
192 (1998), Soria et al. (2013, 2017), Soria (2017) and Mango and Albanesi (2018b).  
193 Moreover, the conodont *O. intermedius* was recorded in the Huanghuachang section  
194 (Wang et al., 2009), South China (Li et al., 2010), Russia (Dubinina and Ryazantsev  
195 2008) and Spitsbergen or the Svalbard Islands (Lehnert et al., 2013).

196 In this contribution, like in those papers of Soria et al. (2013, 2017) and Mango  
197 and Albanesi (2018b), the *Oepikodus intermedius* Zone is considered as an interval  
198 zone. Its lower boundary is indicated by the first occurrence of the eponymous  
199 conodont, and its upper boundary is marked by the first record of the conodont *T. laevis*  
200 or *Triangulodus brevibasis* (Seergeva), which matches with the last occurrence of the  
201 *O. intermedius* (Mango and Albanesi, 2018a,b).

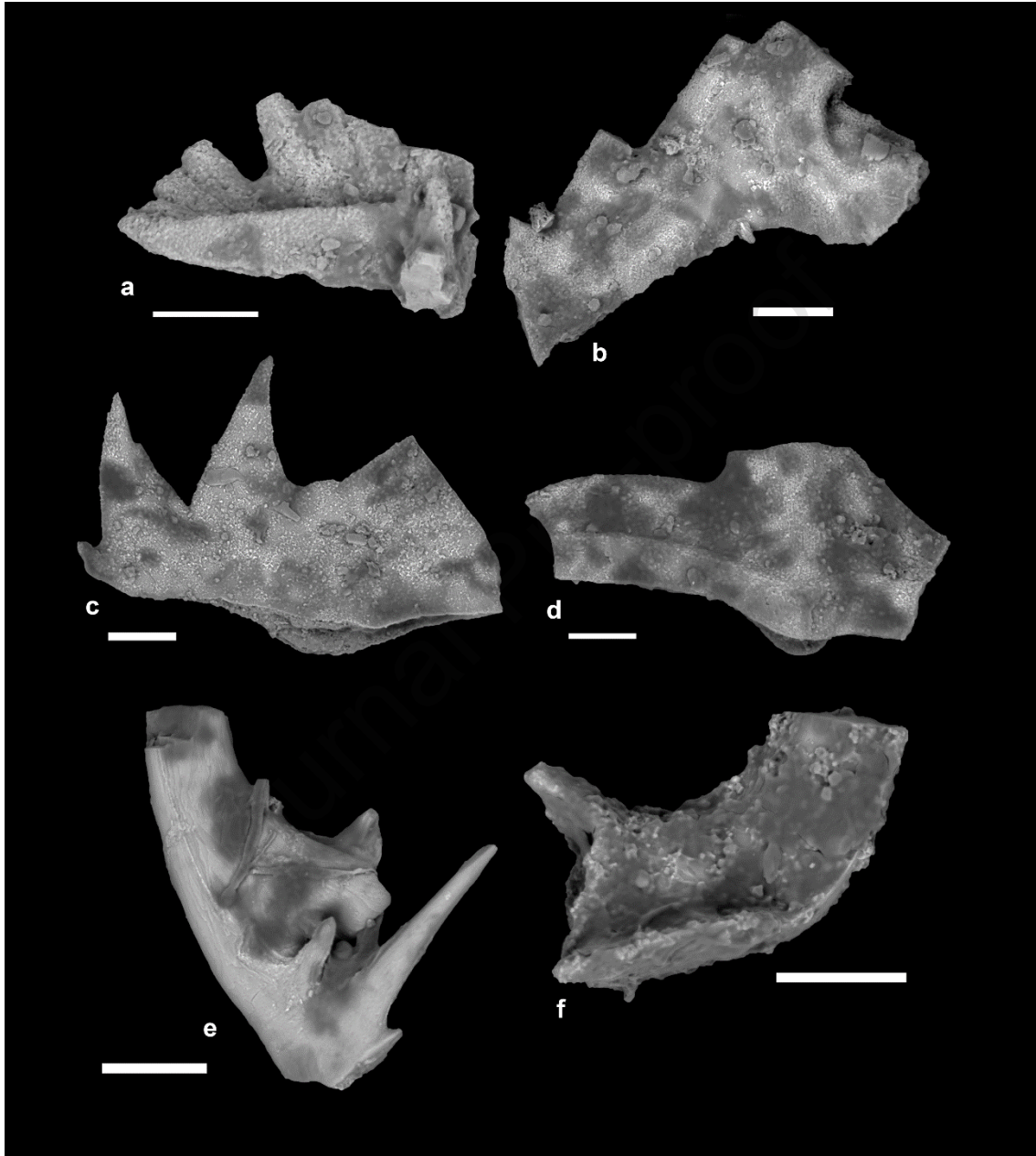
202 The *O. intermedius* Zone may be correlative with the upper part of the *O. evae*  
203 Zone from South China (Wang et al., 2018), the upper part of the *R. andinus* Zone from  
204 North America (Midcontinent) (Ethington and Clark, 1981; Ross et al., 1997), the  
205 *Trapezognathus diprion* and *Microzarkodina* sp. A or upper *O. evae* Zone from  
206 Baltoscandia region (Bagnoli and Stouge, 1997; Viira, 2001), and the upper *O. evae*  
207 Zone from Newfoundland (Johnston and Barnes, 1999) (Fig. 4).

208 The species *B. extensus* has been recorded in North America, China, Australia  
209 and Argentina with an age range equivalent to middle-late Early Ordovician, from the

210 *Prioniodus elegans* to the *O. intermedius* zones (Zhen et al., 2001). Lehnert (1993)

211 extends the upper limit of its biostratigraphic range to the *J. jaanussoni* / *O. aff. O.*

212



213

214 **Figure 3:** Microphotographs of scanning electron microscope. The bar indicates 0.1

215 mm. specimens a-b from Niquivil section and c-f from Talacasto section. (a) *Oepikodus*

216 *intermedius* (Serpagli), Pa element, P sample, INGEO-MP 3573 (1); (b-c)

217 *Bergstroemognathus extensus* (Graves and Ellison), (b) Pb element, P sample, INGEO-

218 MP 3571 (1); (c) S element, T18 sample, INGEO-MP 1953 (1); (d) *Cooperignathus*

219 *aranda* (Cooper), M element, T18 sample, INGEO-MP 1954 (1); (e) *Erraticodon patu*  
220 Cooper, Sc element, T15b sample, INGEO-MP 1851 (4); (f) *Juanognathus variabilis*  
221 (Serpagli), S element, T20 sample, INGEO-MP 1955 (2).

222

223 *lanceolatus* Association which is probably equivalent to the *B. triangularis/B. navis*  
224 Zone. However, Mango and Albanesi (2018a) interpreted that the subsequent conodont  
225 association "*P.*" *nogamii/P. gracilis/A. jemtlandica* Association proposed by Lehnert  
226 (1993) is correlative with the *T. laevis/B. triangularis* Zone, restricting the *B. extensus*  
227 biostratigraphic range to the Early Ordovician as in the worldwide record.

228

#### 229 **4.1 Biostratigraphic discussion**

230 The conodont fauna retrieved from the reef and shoal facies in this contribution  
231 is in agreement with those previously published (Soria et al. 2013; 2017, Mango and  
232 Albanesi, 2018b) and our own conodont data from the middle part of the San Juan  
233 Formation in the Central and Eastern Precordillera sections. However, this new  
234 conodont biostratigraphic data is highly contrasting with the previous conodont  
235 biostratigraphy of this reef facies in the Niquivil section, which was considered as  
236 developed during Dapingian times, *T. laevis* and *B. navis* zones (Albanesi et al., 2003,  
237 2006; Cañas and Carrera, 2003).

238 In the Niquivil section, Albanesi et al. (2003, 2006) verified the first occurrence  
239 of *T. laevis* 20 m below the reef facies from the H1 sample to the N sample, and the  
240 presence of the *B. navis* only in the K sample which is located in the shoal and reef  
241 facies (Albanesi et al., 2006, Fig. 6, 7). On the other hand, Mango and Albanesi (2018a)  
242 in a recent conodont biostratigraphic study in the same section, recorded the first

243 occurrence of *T. laevis* at least 20 m above the reef facies; additionally, these authors  
 244 state the absence of *B. navis* in this section, contrary to the previously registered data by  
 245 Albanesi et al. (2003; 2006). Nevertheless, the incoherence in the record of these  
 246 important index conodonts was not discussed by Mango and Albanesi (2018a).  
 247 Consequently, the late Floian age (*O. intermedius* Zone) recorded here for the reef and  
 248 shoal facies in the Niquivil section is strongly supported by the biostratigraphic  
 249 proposal of Mango and Albanesi (2018a).

250

SERIES	STAGE	South China	Baltoscandia	Newfoundland	North America	Precordillera	
MIDDLE ORDOVICIAN	DARR.	<i>L. variabilis</i>	<i>L. variabilis</i>	<i>Periodon macrodentata</i>	<i>Histiodella sinuosa</i>	<i>L. variabilis</i>	
		<i>L. antivariabilis</i>	<i>B. norrl.</i>			<i>L. antiv.</i>	<i>L. antivariabilis</i>
	DAPINGIAN	<i>M. parva</i>	<i>T. quad.</i>	<i>Periodon hankensis</i>	<i>Histiodella altifrons</i>	<i>M. parva</i>	
		<i>P. originalis</i>	<i>P. originalis</i>			<i>B. navis</i>	
		<i>B. navis</i>	<i>B. navis</i>	<i>Tripodus laevis</i>	<i>Tripodus laevis</i>	<i>T. laevis/ B. triangularis</i>	
		<i>Baltoniodus triangularis</i>	<i>Baltoniodus triangularis</i>				
LOWER ORDOVICIAN	FLOIAN	<i>Oepikodus evae</i>	<i>Microzarkodina sp.A</i>	<i>Oepikodus evae</i>	<i>Reuterodus andinus</i>	<i>Oepikodus intermedius</i>	
			<i>Trapezognathus diprion</i>				<i>Oepikodus evae</i>
			<i>Oepikodus evae</i>				
		<i>Oepikodus communis</i>	<i>Prioniodus elegans</i>	<i>Prioniodus elegans</i>	<i>Oepikodus communis</i>	<i>Prioniodus elegans</i>	
	<i>Prioniodus honghuay.</i>						
	<i>S. diversus</i>	<i>A. deltatus</i>				<i>A. deltatus</i>	

251

252 **Figure 4:** Conodont biostratigraphic correlation across the Lower/Middle Ordovician  
 253 boundary between the Precordillera (Albanesi and Ortega, 2002, Soria et al. 2013, 2017;  
 254 Heredia et al., 2017; Mango and Albanesi, 2018 a, b), South China (Wang et al., 2018),  
 255 Baltoscandia (Bagnoli and Stouge, 1997; Löfgren and Zhang, 2003), Newfoundland  
 256 (Johnston and Barnes, 1999; Stouge, 2012), North America (Ethington and Clark, 1982;

257 Ross et al., 1997). The shadow area shows the study precordilleran reefs age. *A.*,  
258 *Acoudus*; *B.*, *Baltoniodus*; *L.*, *Lenodus*; *M.*, *Microzarkodina*; *P.*, *Paroistodus*; *S.*,  
259 *Serratognathus*; *T.*, *Tripodus*.

260

## 261 **5. Depositional facies**

262 The description of carbonate microfacies is carried out using the classification of  
263 Dunham (1962). Based on textures/fabrics, sedimentary structures, key components and  
264 fossil contents, five microfacies were recognized in the middle part of San Juan  
265 Formation in both sections studied, which represent three genetically - related  
266 depositional facies from distal to proximal, including from shallow subtidal facies  
267 below wave action to shoal banks facies (Table 2).

268

269 **5.1 Facies 1 – Shallow subtidal:** This facies mainly includes greenish nodular  
270 wackestone-packstone (M1) (Fig. 5a-b), it is dominantly thinly irregular to nodular  
271 bedded with thin interbeds of silty shale, and it has a high concentration of gastropods.

272

273 **Nodular biointraclastic wackestone-packstone (M1):** The M1 microfacies is generally  
274 light to medium grey with diverse and abundant robust fauna, and with little evidence of  
275 fossil erosion. The carbonate component consists of gastropods (Fig. 5c-d), calcareous  
276 algae (*Halysis monoliformis*) and calcareous microproblematica (*Nuia sibirica*),  
277 intraclasts, trilobites and brachiopods.

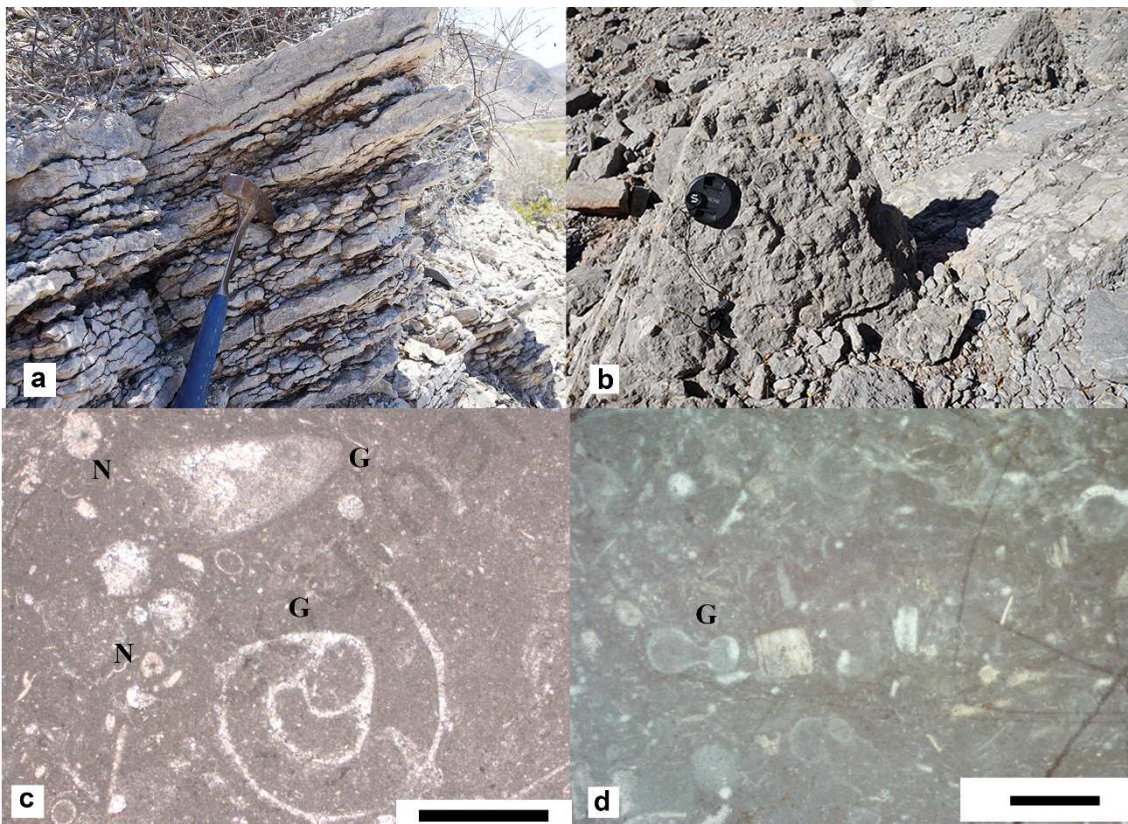
278 The variety of textures, inorganic sedimentary structures, and distribution of  
279 siliciclastics are often obscured by pervasive bioturbation. Based on the diverse faunal  
280 assemblage, limited abrasion of the particles and robust fossil morphologies, as well as



281 the abundance of fine siliciclastic sediment and an intense bioturbation, this facies is  
 282 interpreted as a normal marine shallow subtidal environment below wave action  
 283 (Holland, 1993; Mángano and Droser, 2004). The high concentration of gastropods can  
 284 be used as a paleobathymetric proxy, where the abundance peaks are associated to  
 285 inferred lowstand intervals (Lindskog et al., 2015).

286

287



288

289 **Figure 5 (colour online):** Facies 1, Shallow subtidal below of the wave action. (a)  
 290 Nodular bed outcrop from the Niquivil section, the hammer is 27 cm long. (b) High  
 291 concentration of gastropods on the strata surface, scale represent 6 cm, Talacasto  
 292 section. (c) Photomicrographs of the microfacies M1, (G) gastropods, (N) *Nuia sibirica*,  
 293 scale 1 mm, J sample, Niquivil section. (d) Photograph of a cut slab of the microfacies  
 294 M1, (G) gastropods, scale 0.5 mm, T8 sample, Talacasto section.

295

296

297 **5.2 Facies 2 - Shoal and reef facies:** This facies is dominantly represented by two  
298 microfacies including biointraclastic packstone-grainstone (M2) and Microbial-skeletal  
299 boundstone (M3) (Fig. 6a, c, Fig. 7a-c, Fig. 8a).

300 **Biointraclastic packstone-grainstone (M2):** This microfacies is composed by light to  
301 medium grey fine to very coarse well sorted grainstone. The most common carbonate  
302 components are pelmatozoan ossicles, intraclasts, *Halysis monoliformis* and *Nuia*  
303 *sibirica*, trilobites and brachiopods (Fig. 6b).

304 The stenohaline components dominating microfacies M2 indicate an open marine  
305 environment, with bedding features suggesting common transport and reworking due to  
306 wave action in the inner platform setting. The microfacies could have formed in  
307 extensive coastal shoals or fringing banks (Read, 1985).

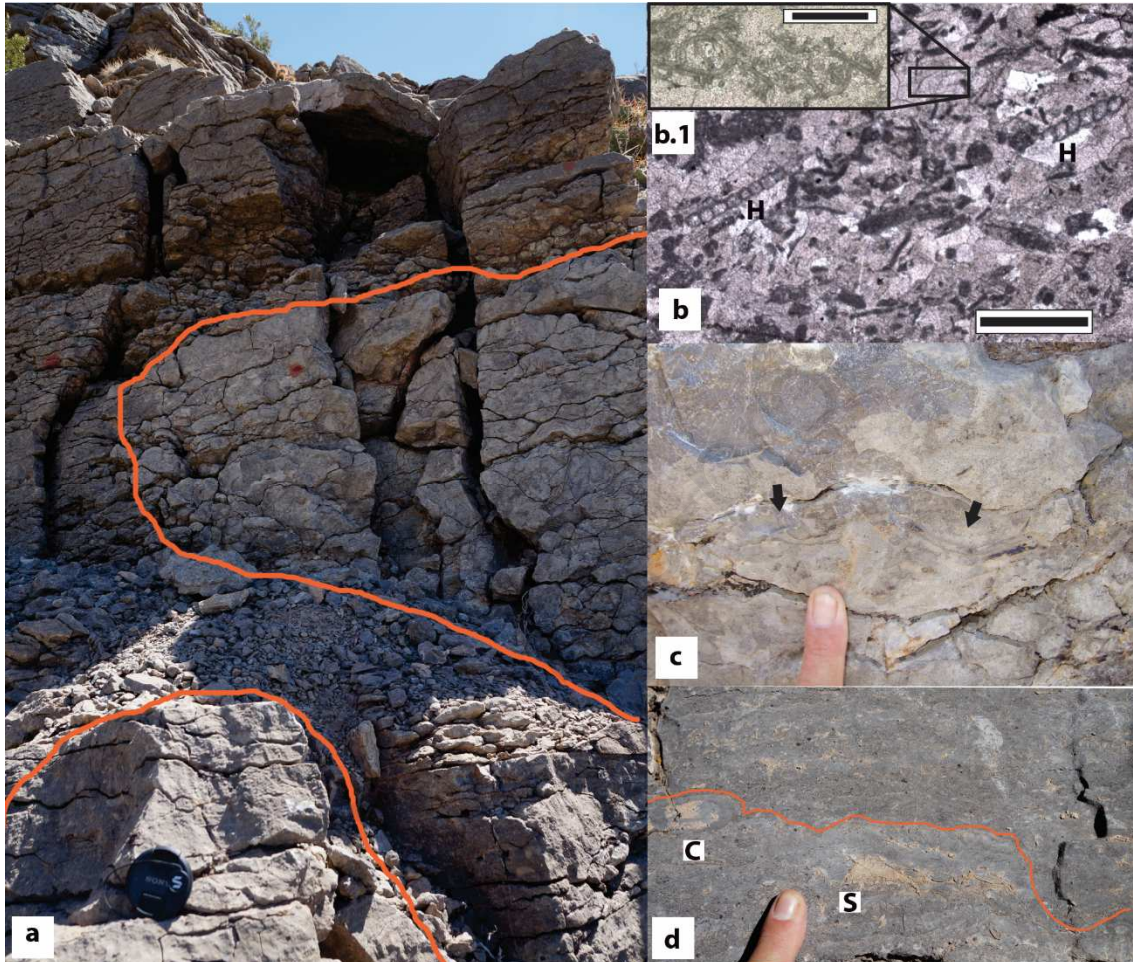
308 **Microbial-Skeletal boundstone (M3):** This microfacies only occurs in the lower levels  
309 studied in the San Juan Formation (Fig. 2) and represents the main microfacies of the  
310 biogenic structure. The reefs components consist of calcimicrobes, pulchrilaminids (*Z.*  
311 *communis*) (Fig. 6c, Fig. 7c-d), lithistid sponges and *Calathium* sp. (Fig. 6d). It also  
312 contains cyanobacteria, calcareous algae, and microproblematica, such as *Girvanella* sp.  
313 *Renalcis?* sp., *N. sibirica*, and *H. monoliformis* (Fig. 8b-c), while brachiopods,  
314 trilobites, nautiloids

315 and pelmatozoan ossicles are poorly represented. Microbes produce soft mats that trap  
316 particulate sediment resulting in matrix-supported reefs (Riding, 1991; 2000; 2002). In  
317 general, this type of reefs consists of a framework of microbes of light grey micrite,  
318 with dispersed pulchrilaminids, *Calathium* sp. and lithistid sponges, conforming cluster  
319 reefs (Riding, 2002) where essentially skeletons in place are adjacent, but not in contact.  
320 The reefs range in shape as they can be small balls, domes and bells (up to 2.5 m in

321 height) with a nodular and laterally discontinuous texture (Fig. 6a, c, Fig. 7a-b, Fig. 8a).

322 The

323



324

325 **Figure 6:** Facies 2, Shoal and reef facies. (a) Outcrop of the relation between M2 and

326 M3 in the Niquivil section, scale represent 6 cm. (b) Photomicrographs of the

327 microfacies M2, (H) *Halysia monoliformis*, scale 1 mm, (b.1) details of *Girvanella* sp.

328 filaments, scale 200 µm, T11 sample. (c) Detail of *Zondarella communis* indicate with

329 black arrow, the finger is 3 cm long. (d) Outcrop of the irregular and diffuse limits

330 between the M1 and M3 in the Talacasto section, (C) *Calathium* sp., (S) sponge, the

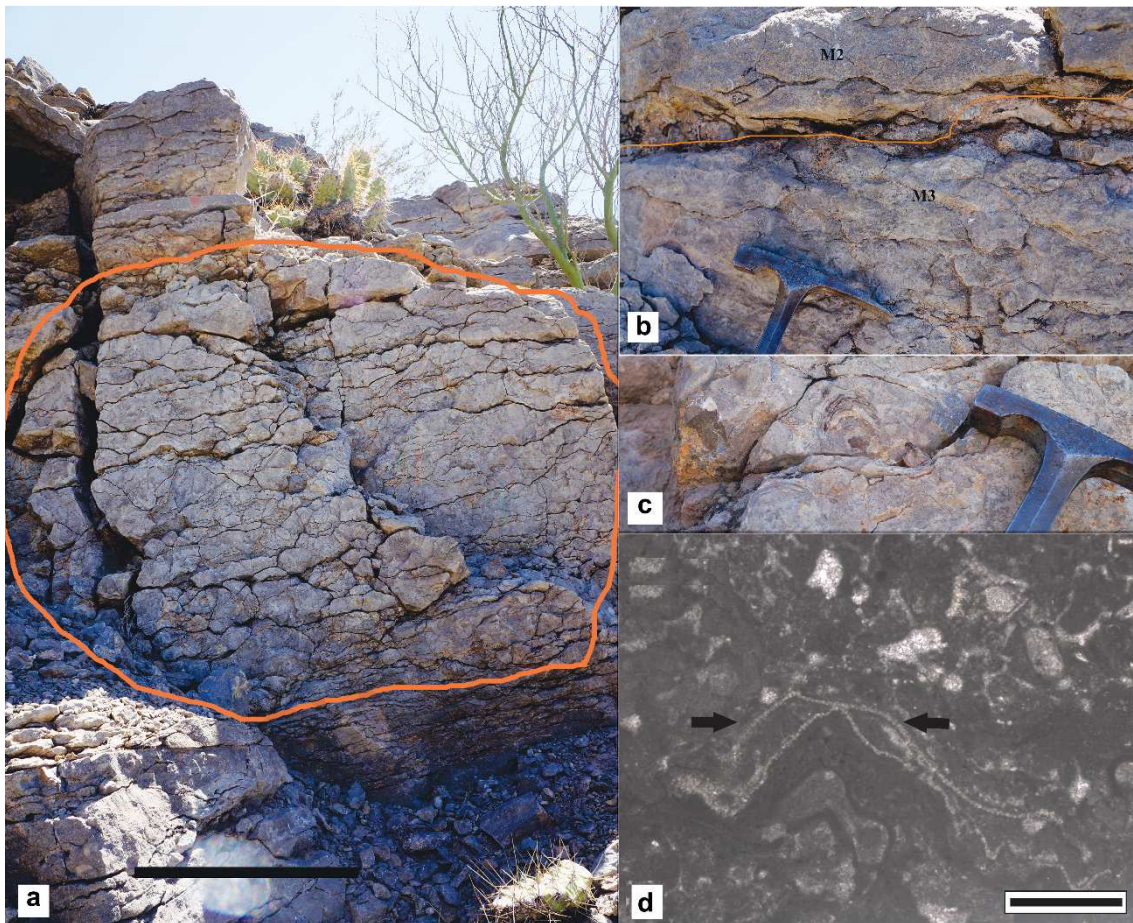
331 finger is 3 cm long.

332

333 microfacies M3 is developed in a shallow subtidal environment, a normal marine setting  
 334 with good circulation, and exposed to intermittent periods of high energy interbedding  
 335 with the M2 microfacies.

336

337



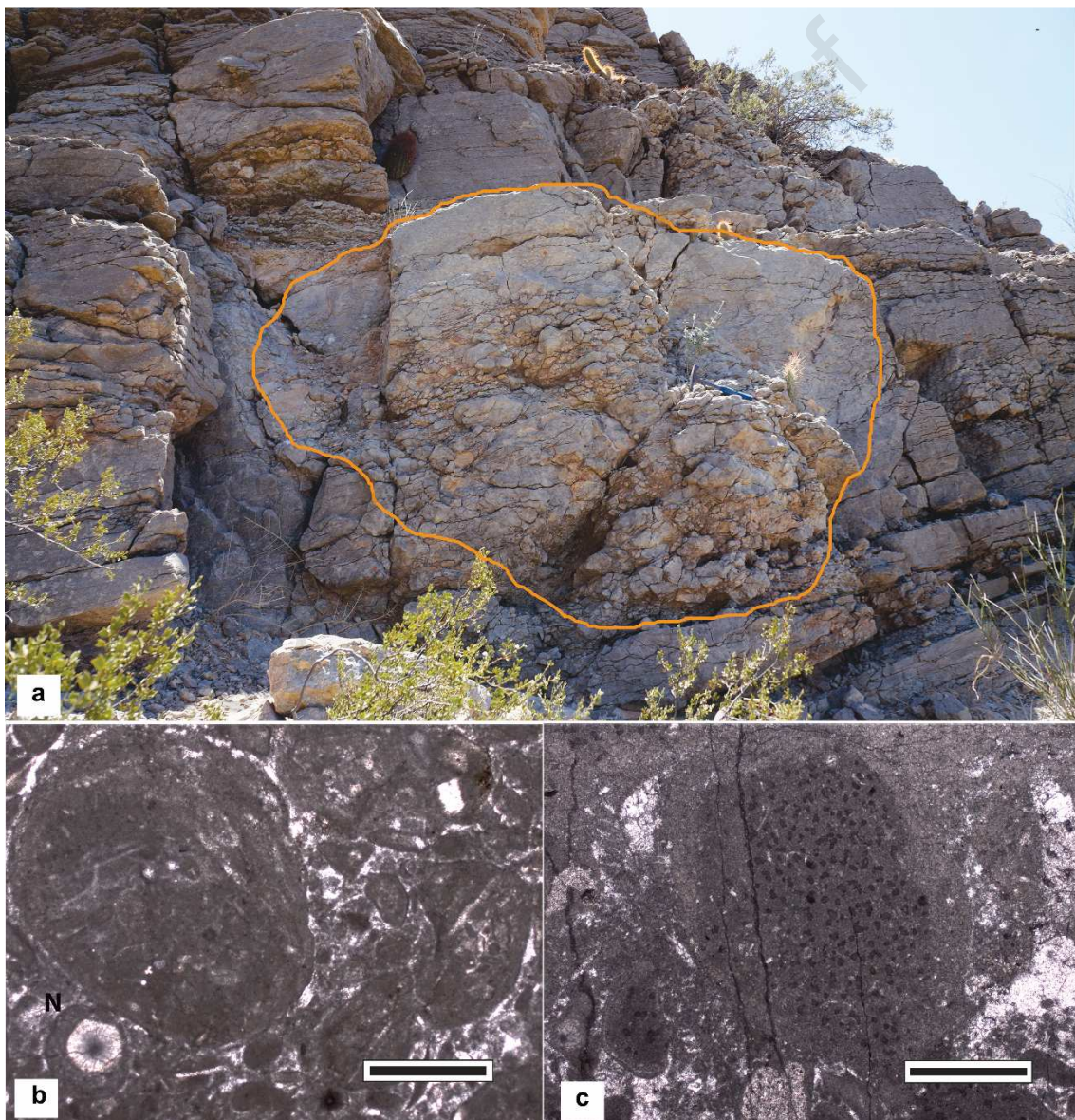
338

339 **Figure 7:** Facies 2 - Shoal and reef facies. (a) Outcrop of the relation between M2 and  
 340 M3, reef with ball-shape, scale represent 1 m, Niquivil section. (b) Outcrop of the clear  
 341 and well-defined limits between the M2 and M3, the hammer is 15 cm long, Niquivil  
 342 section. (c) Detail of *Zondarella communis*, the hammer is 15 cm long, (d)  
 343 Photomicrographs of the microfacies M3, *Zondarella communis* indicate with black  
 344 arrow, scale 1 mm, L sample, Niquivil section.

345 **5.3 Facies 3 - High energy shoal banks:** This facies mainly includes two microfacies,  
346 the intrabioclastic grainstone (M4) and peloidal packstone-grainstone (M5), which  
347 display shallowing-up cycles in the shoal setting with an increase in the amount of  
348 siliciclastic sediment such as lithics and quartz lithoclasts (Fig. 9a-b and Fig. 10a-b).

349

350

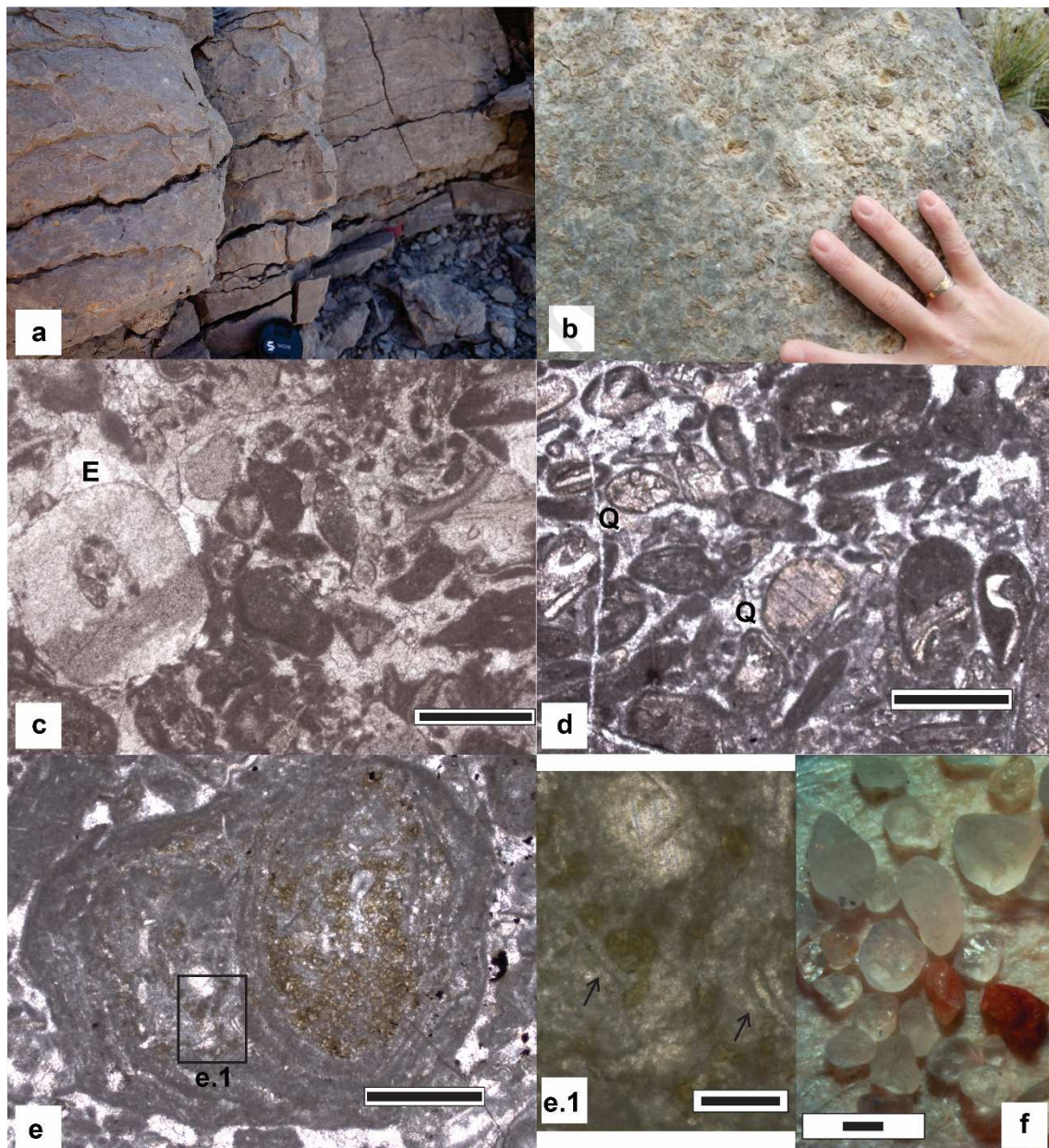


351

352 **Figure 8:** Facies 2 - Shoal and reef facies. (a) Outcrop of the relation between M2 and  
353 M3, reef with bell-shape, the hammer is 27 cm long, Niquivil section. (b)

354 Photomicrographs of the microfacies M3, *Girvanella* sp. balls and (N) *Nuia sibirica*,  
 355 scale 1 mm, T10 sample, Talacasto section. (c) Photomicrographs of the microfacies  
 356 M3, *Girvanella* sp. and *Renalcis?* sp., scale 1 mm, T10 sample, Talacasto section.

357 **Intrabioclastic grainstone (M4):** Microfacies M4 is light to reddish grey in color with  
 358 thin to very thick tabular beds, erosive base and sharp top in amalgamated and stacked  
 359



360

361 **Figure 9 (colour online):** Facies 3 - High energy shoal banks. (a) Outcrop of the  
 362 amalgamated and stacked beds, Niquivil section, scale represent 6 cm. (b) High

363 concentrations of pelmatozoan ossicles and articulate stems on the strata surface in the  
364 Talacasto section, the finger is 7 cm long. (c) Photomicrograph of the microfacies M4,  
365 (E) pelmatozoan ossicles and intraclast, scale 1 mm, P sample, Niquivil section. (d)  
366 Photomicrographs of the microfacies M4, intraclast and (Q) quartz lithoclast, scale 1  
367 mm, T14 sample, Talacasto section. (e) Photomicrographs of the microfacies M4,  
368 *Girvanella* sp. oncoids, scale 1 mm, (e.1) details of *Girvanella* sp. filaments, scale 200  
369  $\mu\text{m}$ , T15b sample, Talacasto section. (f) Quartz and lithic lithoclast recovered from  
370 insoluble residue of conodont process, scale 0.5 mm, T14 sample, Talacasto section.

371 beds. It comprises intraclasts, pelmatozoan ossicles (Fig. 9c), *Girvanella* sp., oncoids  
372 (Fig. 9e), lithoclasts (Fig. 9d, f), *Calathium* sp., sponges, brachiopods, bryozoans, and  
373 bioclastic fragments, with moderately to grain-supported and well-sorted textures.  
374 Diagenetic chert and iron oxide staining bioclasts are also observed.

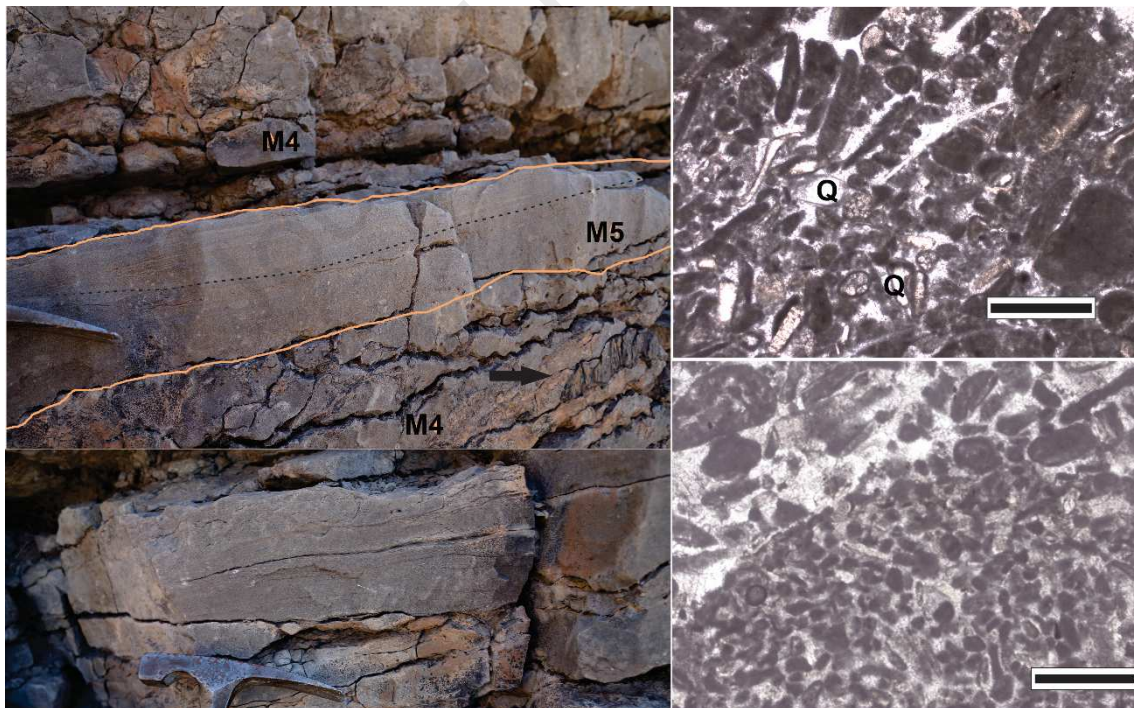
375 The dominating stenohaline pelmatozoans indicate an open marine environment  
376 suggesting common reworking and transport due to wave action. This largely encrinitic  
377 facies represents extensive pelmatozoan meadows, whose sediment was locally  
378 reworked into shoal banks and bars by wave action and/or storm events (Aigner, 1985;  
379 Ausich, 1997; Batten Hender and Dix, 2008). The oncoids in this microfacies rarely  
380 exceed 2 mm in size and show a range of shapes, with nuclei of particles encrusted with  
381 asymmetric sets of crinkly and thinly laminated micrite, or with slightly denser layers of  
382 *Girvanella* filaments forming a laminated or meshwork fabric. The sets of laminae are  
383 frequently disconformable, likely indicating episodic rotation of oncoids (Fig. 9E)  
384 (Batten Hender and Dix, 2008). Many intraclasts and bioclasts within this facies possess  
385 brownish rust-stained margins encrusted by *Girvanella* (Fig. 9c-d).

386

387 ***Peloidal packstone-grainstone (M5)***: This microfacies is mainly light grey to grey in  
 388 color, and it shows thin to medium tabular beds. It consists predominantly of  
 389 moderately-sorted peloids, and it has minor bioclasts and intraclasts. It displays sharp-  
 390 erosive bases and burrowed tops, planar lamination and low-angle cross-stratification  
 391 (Fig. 10A-B). Iron oxide nodules are developed on the strata surfaces. Rare fossil  
 392 fragments of pelmatozoan, brachiopods and trilobites are present.

393 The presence of planar lamination and low-angle cross-stratification with well-  
 394 sorted peloids is dominant over the grain-supported textures (Fig. 10c-d). This indicates  
 395 high-energy and wave-agitated environments during deposition conforming shoal banks  
 396 and bars (Batten Hender and Dix, 2008; Hamon and Merzeraud, 2008; Zhang et al.,  
 397 2015a,b; Chen et al., 2016; Gou et al., 2018).

398



399

400 **Figure 10:** Facies 3 - High energy shoal banks. (a-b) Outcrop of the thin to medium  
 401 tabular beds, with sharp-erosive bases, planar lamination and low-angle cross-  
 402 stratification, (a) scale represent 6 cm. (b) the hammer is 15 cm long. (c-d)



403 Photomicrographs of the microfacies M5, peloids and (Q) quartz lithoclast, scale 1 mm.  
404 (c) T16 sample, Talacasto section. (d) N sample, Niquivil section.

405

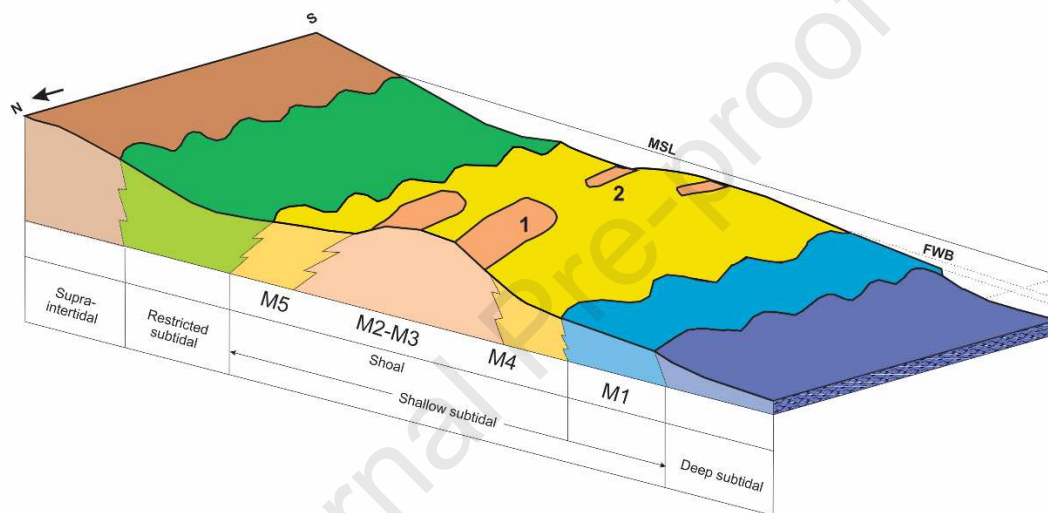
## 406 **6. Comparison between the Niquivil shoal and reef facies and the Talacasto** 407 **equivalent beds**

408 In recent years, many authors have made contributions about Ordovician reef  
409 and shoal facies providing extensive discussions and new ideas on the origin,  
410 distribution and composition of the facies and reef frame-organisms (Adachi et al.,  
411 2011; Carrera et al., 2017; Hong et al., 2017; Li et al., 2015, 2017, 2018, among others).  
412 The most recent contribution about these topics from the Precordillera was that of Cañas  
413 and Carrera (2003) who studied the La Silla, Niquivil and San Roque sections from the  
414 Central Precordillera.

415 The Niquivil section is here restudied in order to compare it to the Talacasto  
416 section for first time, showing differences in the distribution, morphology and fauna  
417 composition in the shoal and reef facies (Fig. 2). Moreover, the comparison between  
418 them allows the recognition of subtle variations in the environment conditions during  
419 the growth of the reefs.

420 The stratigraphic levels analyzed in the Niquivil section are 40 m thick, whereas  
421 in the Talacasto section is 38 m thick (Fig. 2). The reefs facies are embedded in the base  
422 of the shoals (biointraclastic packstone-grainstone) in both sections. The Niquivil reefs  
423 present variable dimensions from 2.5-3.5 m in width and 1.5-2.5 m in height, with clear  
424 and well-defined limits (Fig. 6a, Fig. 7a-b and Fig. 8a), whereas the size in the  
425 Talacasto reefs varies from 0.5-1 m in width and 1-1.5 m in height, and the limits are  
426 irregular and diffuse (Fig. 6d).

427 The skeletal components observed in the Niquivil reef facies consist specially by  
 428 *Zondarella communis*, *Calathium* sp., sponges, whereas nautiloids, gastropods,  
 429 brachiopods, trilobites and pelmatozoan ossicles are scarce. On the other hand, the  
 430 Talacasto reef facies is characterized by sponges (as main component) and *Calathium*  
 431 sp. The *Zondarella communis* specimens are small and scarce as well as the  
 432 brachiopods, gastropods, trilobites and pelmatozoan ossicles, which are rare or absent.  
 433



434  
 435 **Figure 11:** Carbonate platform depositional model for the San Juan Formation in the  
 436 study areas. The platform displays a gentle transition from shallow to deeper  
 437 depositional environments. The subdivision of the carbonate platform is based on  
 438 Pomar (2001). FWB- fair-weather wave base, MSL – medium sea level, 1- Niquivil, 2-  
 439 Talacasto sections.

440

441 A detailed study of the framework of the reef facies and its relation to the reef-  
 442 builder organism should be carried out in the future in order to resolve the interaction  
 443 between the reef-builders and the real nature of the *Zondarella communis*, due to the  
 444 fact that the latter is interpreted as pulchrilaminids (Webby, 2012) or by microbial  
 445 generation, like stromatolite (Cañas and Carrera, 2003).

446 In the present report, a comparative analysis of reef and shoal facies between the  
447 Niquivil and Talacasto sections is developed in order to show that the differences  
448 between these reef communities were essentially controlled by the bathymetry and  
449 morphology of the platform (Fig. 11). Although sea-level fluctuation is an important  
450 variable that controls regional reef development, it is estimated that energy change is a  
451 first-order factor that controls reef growth (Zhang et al., 2015b, 2016). Based on this  
452 statement we interpret a probable shallower depositional environment in the Niquivil  
453 section compared to the Talacasto section.

454

## 455 **7. Depositional model and environmental significance**

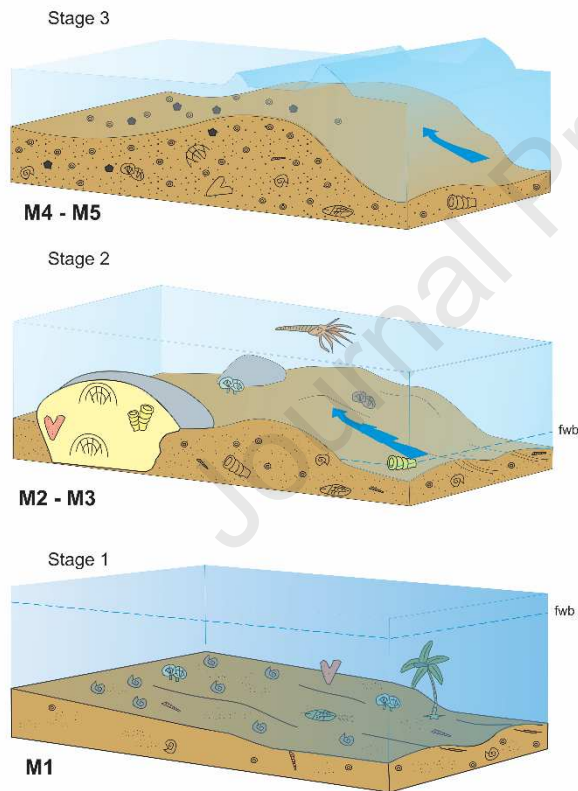
456 The vertical distribution of the facies and microfacies in the middle part of San  
457 Juan Formation in the Talacasto and Niquivil sections and their arrangement from  
458 shallow subtidal below wave action to shoal and reef settings, suggest that these beds  
459 represented an open-ocean, relatively high-energy carbonate platform, and denote that  
460 their shallowest depositional position occurred in the upper *O. intermedius* Zone  
461 (uppermost Floian). Therefore, it is possible to recognize three evolutionary stages in  
462 the build of the shoal banks.

463 Stage 1 (Fig. 12) is represented by Facies 1 (Nodular biointraclastic wackestone-  
464 packstone) where the high fauna diversity, the intensity of bioturbation and the  
465 interbedding fine silty shale observed in this facies, suggest low energy conditions in  
466 the subtidal environment below the fair water wave base in the photic zone due to the  
467 presence of *H. monoliformis* and *N. sibirica*.

468 Gradual regression during Stage 2 (Fig. 12) is represented by Facies 2, where the  
469 increase of the wave action produced the intraclast and bioclast reworking in this

470 deposit characterized by the biointraclast packstone-grainstone microfacies (M2). The  
 471 accumulation of carbonate material by wave action building shoal bars presumably  
 472 parallel to the shoreline in the inner platform settings (Flügel, 2010) generated  
 473 protection and a relatively shallow environment. In these conditions, the reef grew on  
 474 the shoals, and its framework consisted of open microbialites colonies with *Zondarella*  
 475 *communis*, *Calathium* sp. and sponges as reef-builders (M3 microfacies). The spaces  
 476 between this organic framework were filled by carbonate mud, giving as a result matrix-  
 477 supported reefs (Riding, 1991; 2000; 2002).

478



479

480 **Figure 12:** Dynamic facies model, showing distribution of facies and timing of the  
 481 arrangement from shallow subtidal below wave action to reef and shoal, recognizing  
 482 three evolutionary stages in the built of the shoal banks (for legends see Fig. 2).

483 The reefs of the San Juan Formation could have formed in 6 to 12 m water  
 484 depths due to the presence of *Calathium* sp. (Nitecki 1972; Kaya and Friedman, 1997),

485 in a normal marine environment with good circulation, and subjected to intermittent  
486 periods of high energy in the shallow subtidal shoal setting.

487 Subsequently, the gradual increase of energy in shallower environments  
488 produced that the reefs were covered by coarse carbonate and lithic material developing  
489 high energy shoal banks represented by Facies 3 (Stage 3, Fig. 12). The microfacies M4  
490 and M5 are interbedding and they conform the thickest facies in the stratigraphical  
491 levels studied.

492 Recent studies have attempted to calibrate the absolute depths of the lithofacies  
493 and biofacies in a well-constrained Upper Ordovician stratigraphic interval of the  
494 classic Cincinnati Arch region (northern Kentucky and southern Ohio), indicating the  
495 orientation and gradient of an ancient gently dipping carbonate ramp (Brett et al., 2015).  
496 The conclusion was that the cross-bedded grainstone that represent shoal-type  
497 environments are within the 6 - 18 m depth range, in agreement with estimates of  
498 normal wave base in epeiric seas which is of 5 - 15 m (Brett et al., 1993).

499 A regression trend is recognized in the shoal and reef facies from the  
500 Precordillera, which is composed by successions of coarsening-up and thickening-up  
501 strata that reflects a gradual shallowing-upward evolution during the *O. intermedius*  
502 Zone (late Floian).

503

## 504 **8. Paleogeographic significance of the Precordilleran late Floian shoal and reef** 505 **facies**

506 The late Floian (late Early Ordovician) regression trend registered in the shoal  
507 and reef facies studied here has already been documented by Nielsen (2003, 2011) and  
508 Haq & Schutter (2008) for Baltoscandia and Laurentia. Nielsen (2003) proposed an

509 abruptly sea-level lowering in this time interval, the Latest Billingen Stage  
510 (Baltoscandian) or Basal Whiterock (Laurentia) after the *Evae* highstand cycle. This  
511 regression event is recorded in other regions where the carbonate and siliciclastic coarse  
512 deposits were developed. Agematsu and Sashida (2009) registered late Floian (*T.*  
513 *larapintinensis* Zone) shoal to backshoal deposits from the Sibumasu Terrane  
514 (Thailand), and Astini et al. (2004) verified a late Floian deltaic progradation to the top  
515 of the Acoite Formation in the Eastern Cordillera during the *T. diprion-* *B. cf.*  
516 *triangularis* Zone (Carlorosi et al., 2013).

517 An overview of the Precordilleran Ordovician reefs was made by Cañas and  
518 Carrera (2003) proposing three reef types: 1- Thrombolithic reef dominating during the  
519 Upper Cambrian and the of most Tremadocian; 2- Microbialite-metazoan reef in the late  
520 Tremadocian; 3- Microbialite-*Zondarella-Calathium* reef and *Zondarella*-dominated  
521 reef in the early Middle Ordovician (Dapingian). These two types of Middle Ordovician  
522 reefs are present in different regions of the Precordillera. The Microbialite-*Zondarella-*  
523 *Calathium* reef is located in the Central Precordillera, and the *Zondarella*-dominated  
524 reef has been described for the Eastern Precordillera (Cañas and Carrera, 2003). These  
525 authors considered a microbial origin for *Zondarella*, opposed to the interpretation  
526 proposed by Keller and Flügel (1996), Stearns et al. (1999), Zhen and Pickett (2008),  
527 Webby (2012) and Hong et al. (2018). In the present contribution the followed criterion  
528 is that proposed by Webby (2012) who consider *Zondarella* as Pulchrilaminid  
529 (hypercalsified sponges).

530 The reef facies studied in the present report coincides with the Microbialite-  
531 *Zondarella-Calathium* reef proposed by Cañas and Carrera (2003). However, the new  
532 biostratigraphic and sedimentologic information allows indicating an accurate late  
533 Floian age (later *O. intermedius* Zone) for the reef facies, improving the knowledge of

534 paleoenvironmental and paleogeographic distribution of the pulchrilaminid (*Z.*  
535 *communis*) for this time interval.

536 The conodont information from the *Zondarella*-dominated reefs (Eastern  
537 Precordillera) reports that these reefs appear immediately below carbonate beds that  
538 represent at least the *Lenodus variabilis* Zone (Mestre, 2014; Heredia et al., 2017) or  
539 more likely the *L. antivariabilis* Zone (Heredia and Mestre, 2017), proposing a latest  
540 Dapingian to earliest Darriwilian age (Fig. 13) for these reefs, in agreement with the  
541 previous age suggested by Lehnert and Keller (1993).

542 Cañas and Carrera (2003) suggested that the San Juan Formation reef sequences  
543 correspond to the globally recognized reef-forming phases 1 to 3 proposed by Webby  
544 (2002). Nevertheless, the Middle Ordovician reefs correspond to phase 4, which  
545 includes Dapingian-Early Darriwilian reefs. We propose that the Microbialite-  
546 *Zondarella-Calathium* reef corresponds to the upper part of the phase 3 and the  
547 *Zondarella*-dominated reef to the upper part of the phase 4 (Fig. 13). The new  
548 biostratigraphic location of the Precordilleran pulchrilaminids (*Z. communis*) provides a  
549 new insight on the paleogeographic distribution of this restricted group of “hypercal-  
550 cified sponges”.

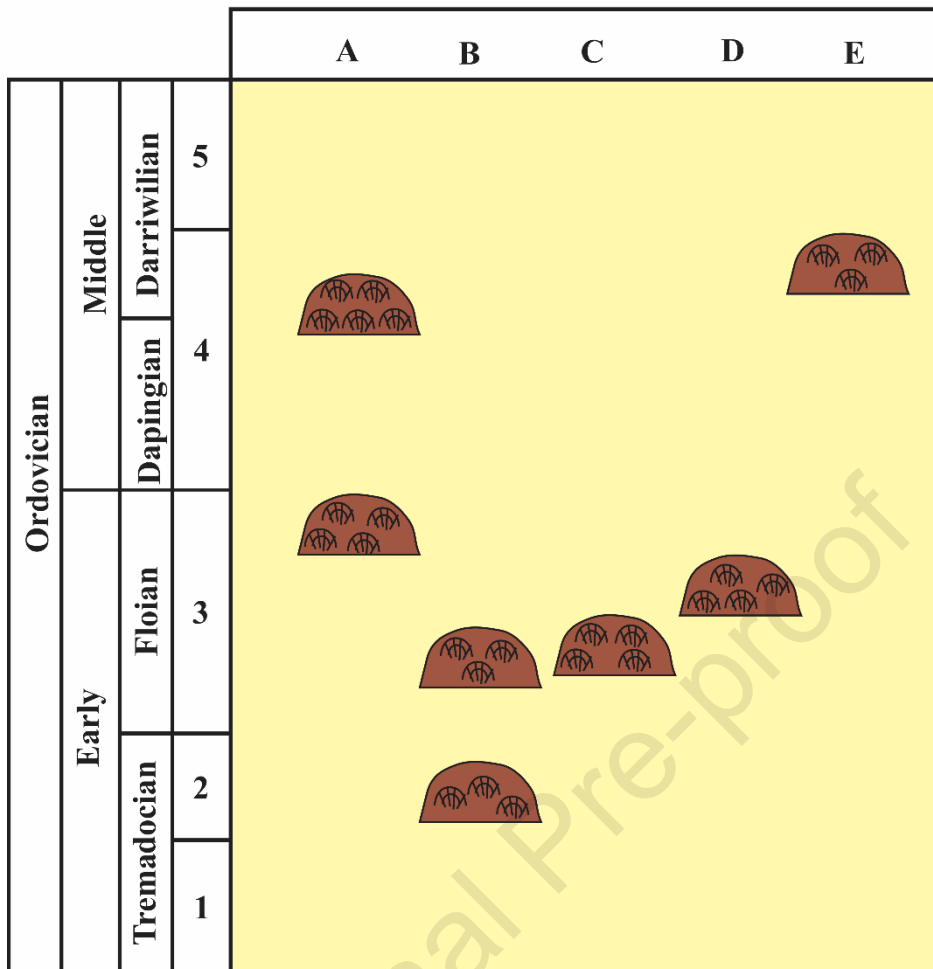
551 The oldest encrusting pulchrilaminid (genus *Pulchrilamina*) was reported from  
552 the Tremadocian to the early Floian in the provinces of Hubei and Guizhou, South  
553 China (Zhu et al., 1993; Adachi et al., 2011) (Fig. 13, 14). The *Pulchrilamina* have also  
554 been recorded in North America (in the states of Texas and Oklahoma) from early  
555 Floian strata, where they are the main framework-builders exhibiting large domical  
556 forms (Toomey and Ham, 1967; Toomey, 1970; Toomey and Nitecki, 1979; Toomey  
557 and Babcock, 1983; Webby, 1986, 2002) (Fig. 12, 13). Moreover, this genus was

558 reported in Newfoundland from early Floian strata (Pratt & James, 1989) (Fig. 13, 14)  
559 and reef-derived clasts of probable Floian-Dapingian age (Pohler and James, 1989) that  
560 were not taken in consideration due to their reworked origin.

561 The youngest record of pulchrilaminids as that proposed by Webby (2012), is  
562 represented by *Ianilamina kirkupensis* Pickett and Zhen, from the central New South  
563 Wales (Australia), as an isolated occurrence in early Darriwilian limestone lens related  
564 to a volcanic arc setting. Zhen and Pickett (2008) inferred that *Ianilamina kirkupensis* is  
565 the most similar species compared to *Z. communis* from Argentina (Keller and Flügel  
566 1996). The main differences between them are the well-developed pores in the laminae  
567 of the *Ianilamina* that have not been observed in *Zondarella*. However, the frequent  
568 disruption in the laminae of this former species could be equal to the *Ianilamina* pores,  
569 and the presence of encrusting bryozoan in both species allow a close comparison  
570 between them (Zhen and Pickett, 2008).

571





572

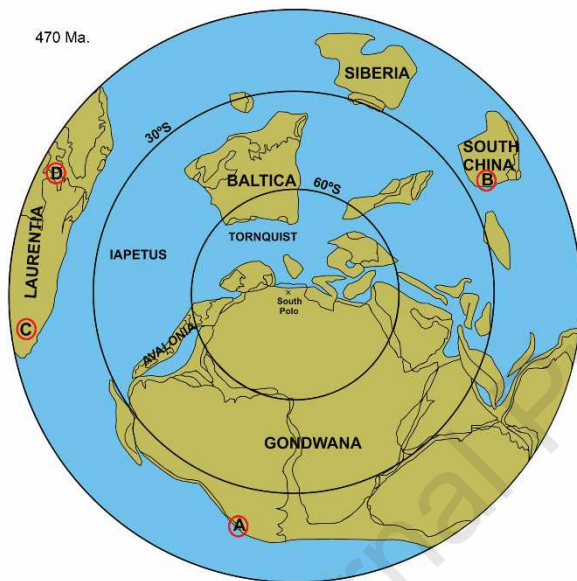
573 **Figure 13:** Scheme of vertical distribution of the Early-Middle Ordovician  
 574 pulchrilamiloïd reefs and its location in the division of Webby (2002) of the Ordovician  
 575 reef-building phases. A- Precordillera (this study); B- South China (Zhu et al., 1993;  
 576 Adachi et al., 2011); C- North America (Toomey and Nitecki, 1979; Toomey and  
 577 Babcock, 1983); D- Newfoundland (Pratt and James, 1989); E- Australia (Zhen and  
 578 Pickett, 2008).

579 The late Floian pulchrilaminids from the Precordillera represent the youngest  
 580 record of this reef-builder organism in the Early Ordovician (Fig. 13, 14). The latest  
 581 Early Ordovician time was interpreted by Webby (2012) as a doubtful evolutionary  
 582 period for Early Ordovician pulchrilaminids. This new record provides crucial  
 583 information on early skeletal reefs, increasing the knowledge for the reconstruction of

584 the evolutionary trends of these reef-builder organisms and their distribution during the  
 585 Early and Middle Ordovician on the western margin of Gondwana.

586 Another important datum verified here is the increasing lithic input from the  
 587 base to the top in the shoal facies. The size, shape and composition of the lithics (Fig.  
 588 9f) allow inferring a mature and relatively proximal continental area of provenance.

589



590

591 **Figure 14:** Global distribution of Early Ordovician pulchrilaminid reefs. A-  
 592 Precordillera; B- South China; C- North America; D- Newfoundland. (Modified from  
 593 Cocks and Torsvik, 2002).

594 The Precordillera is considered as an allochthonous terrane that docked to the  
 595 western margin of Gondwana during Middle Ordovician (Benedetto, 1993; Astini et al.,  
 596 1995; Thomas and Astini, 1996, 1999; Thomas et al., 2002). The allochthonous model  
 597 is supported, between other arguments, by a progressive change in biogeographic  
 598 affinities of the Precordilleran fauna from the late Cambrian to the Ordovician times,  
 599 from entirely Laurentian fauna to mainly Gondwanan fauna. On the basis of the  
 600 variations in the proportion of Laurentian to Gondwanan elements, four biogeographic

601 evolution stages were proposed for the Precordillera terrane (Benedetto et al., 1999).  
602 They are: Laurentian stage (Cambrian-Tremadocian), isolation stage (Floian-  
603 Dapingian), pre-accretion stage (Darriwilian-Katian), and finally the Gondwanan stage  
604 (Hirnantian-Silurian). The isolation stage was achieved when the Precordillera was  
605 disconnected from the Laurentian continental margin and before it reached the  
606 continental margin of Gondwana. The abundance and type of lithoclasts recovered from  
607 the shoal facies during the supposed isolation stage would suggest the connection to a  
608 mature continent during the late Floian.

609

## 610 **9. Conclusions**

611 This research implicated an integral analysis of field observations, thin sections, and  
612 conodont biostratigraphic data, in order to study the facies, depositional environment  
613 and accurate age of the San Juan Formation middle part shallow facies that was  
614 deposited during the Early Ordovician in the Central Precordillera. The conclusions are  
615 summarized as follows:

- 616 • Three facies and five microfacies were recognized in the Talacasto and Niquivil  
617 sections, which represent three genetically-related depositional facies from distal  
618 to proximal, including from shallow subtidal facies below wave action to shoal  
619 and reef facies.
- 620 • A regression trend is recognized in the Precordilleran shoal bank setting,  
621 composed by a succession of coarsening-up and thickening-up strata that reflects  
622 a gradual shallowing-upward evolution during the *O. intermedius* Zone.
- 623 • The reef facies is recognized for the first time at the Talacasto section,  
624 representing the most southern record of this facies from the Central  
625 Precordillera.

- 626 • The reefs consist of a microbial micrite framework in consortium with  
627 *Zondarella communis* (pulchrilaminids), *Calathium* sp. and sponges, conforming  
628 microbial-metazoan matrix-supported reefs.
- 629 • A comparison between the shoal and reef facies from the Talacasto and the  
630 Niquivil sections is presented for the first time. The differences between the reef  
631 communities led to infer a probable shallower depositional environment in the  
632 Niquivil section compared to the Talacasto section.
- 633 • The pulchrilaminid (*Zondarella communis*) present in these reef facies is  
634 accurately assigned for the first time to the *Oepikodus intermedius* Zone,  
635 indicating a late Floian age for this reef-building organism.
- 636 • The record of this Precordilleran pulchrilaminids represents the youngest  
637 evidence for this reef-framer organism compared to the worldwide records of the  
638 Early Ordovician age.
- 639 • In a global context, the pulchrilaminid reefs from the San Juan Formation match  
640 phases 3 and 4 of Webby's (2002) division of Ordovician reef-building phases.
- 641 • The present study of the Precordilleran Early Ordovician reefs increases the  
642 knowledge about the dispersal pathways of the pulchrilaminids during the  
643 Ordovician, and provides crucial information for understanding the  
644 paleogeographic reconstruction of the western margin of Gondwana in the  
645 Early Ordovician.

#### 646 **Acknowledgements**

647 The authors wish to thank the CONICET (National Research Council of  
648 Argentina) to support this contribution through the grant PIP 2014 0058CO. We are  
649 thankful to Qi-Jian Li and Ian Percival for their constructive revision and comments on

650 the manuscript which greatly improved the quality of this article. AM is also sincerely  
651 grateful to Romina Atencio for your assistance in the language improvement of the  
652 manuscript. This is a contribution to the International Geoscience Program (IGCP)  
653 Project 653 – The onset of the Great Ordovician Biodiversification Event. This study  
654 was based on the Graduate Thesis of Lic. Leandro Benegas and Andres Morfil, San  
655 Juan University, Argentina.

656

## 657 **References**

658 Adachi, N., Ezaki, Y., Liu, J., 2011. Early Ordovician shift in reef construction from  
659 microbial to metazoan reefs. *Palaios* 26, 106-114.

660 Adachi, N., Liu, J., Ezaki, Y., 2012. Early Ordovician stromatoporoid *Pulchrilamina*  
661 *spinosa* from South China: geobiological significance and implications for the early  
662 development of skeletal-dominated reefs. *Paleontological Research* 16, 59-69.

663 Agematsu, S., Sashida, K., 2009. Ordovician sea-level change and paleogeography of  
664 the Sibumasu terrane based on the conodont biostratigraphy. *Paleontological Research*  
665 13, 327-336.

666 Aigner, T., 1985. Storm depositional systems: dynamic stratigraphy in modern and  
667 ancient shallow-marine sequences. In: *Lecture Notes in Earth Sciences 3* (eds. G.,  
668 Friedman, H. Neugebauer, A. Seilacher,), pp.1-174, Springer-Verlag, Berlin.

669 Albanesi, G., Hünicken, M., Barnes, C., 1998. Bioestratigrafía de conodontes de las  
670 secuencias ordovícicas del cerro Potrerillo, Precordillera Central de San Juan, R.  
671 Argentina. *Academia Nacional de Ciencias, Córdoba*, XII, 1-72.

- 672 Albanesi, G.L., Carrera, M.G., Cañas, F.L., Saltzman, M.R., 2003. The Niquivil  
673 Section, Precordillera of San Juan, Argentina, proposed GSSP for the Lower/Middle  
674 Ordovician boundary. In: Ordovician from the Andes. Proceedings of the 9th  
675 International Symposium on the Ordovician System (eds. G.L, Albanesi, M.S., Beresi &  
676 S.H., Peralta), pp. 30-44, INSUGEO, Serie Correlación Geológica 17, Tucumán.
- 677 Albanesi, G.L., Carrera, M.G., Cañas, F.L., Saltzman, M. R., 2006. A proposed global  
678 boundary stratotype section and point (GSSP) for the base of the Middle Ordovician  
679 Series: The Niquivil section, Precordillera of San Juan, Argentina. Episodes 29, 1-15.
- 680 Astini, R.A., 2003. The Ordovician Proto-Andean basins. In *Ordovician fossils of*  
681 *Argentina* (ed. J.L., Benedetto) pp. 1-74, Secretaría de Ciencia y tecnología,  
682 Universidad Nacional de Córdoba.
- 683 Astini, R.A., Benedetto, J.L., Vaccari, N.E., 1995. The early Paleozoic evolution of the  
684 Argentina Precordillera as a Laurentian rifted, drifted, and collided terrane: a  
685 geodynamic model. Geological Society of American Bulletin, Colorado. Special Paper  
686 107, 253-273.
- 687 Astini, R.A., Davila, Em., Rapela, C.W., Pankhurst, R.J., Fanning, C.M., 2003.  
688 Ordovician back-arc clastic wedge in the Famatina Ranges: new ages and implications  
689 for reconstruction of the proto-andean Gondwana margin. In: Ordovician from the  
690 Andes (eds. G.L, Albanesi, M.S., Beresi & S.H., Peralta), pp. 375-380, INSUGEO,  
691 Serie Correlación Geológica 17, Tucumán.
- 692 Ausich, W.I., 1997. Regional encrinites: a vanished lithofacies. In: Paleontological  
693 events: stratigraphic, ecological, and evolutionary implications (eds. C.E., Brett & G.C.  
694 Baird), pp. 509–519, Columbia University Press, New York.

- 695 Bagnoli, G., Stouge, S., 1997. Lower Ordovician (Billingenian–Kunda) conodont  
696 zonation and provinces based on sections from Horns Udde, north Öland, Sweden.  
697 *Bolletino della Società Paleontologica Italiana* 35, 109–63.
- 698 Baldis, B.A., Bordonaro, O.L., Beresi, M., Uliarte, E., 1981. Zona de dispersión  
699 estromatolítica en la secuencia calcáreo dolomítica del Paleozoico inferior de San Juan.  
700 8° Congreso Geológico Argentino, Actas 2, pp. 419-434.
- 701 Baldis, B., Beresi, M., Bordonaro, O., Vaca, A., 1982. Síntesis evolutiva de la  
702 Precordillera Argentina. V Congreso Latinoamericano de Geología, Buenos Aires,  
703 Actas IV, pp. 399-445.
- 704 Batten Hender, K.L., Dix, G.R., 2008. Facies development of a Late Ordovician mixed  
705 carbonate-siliciclastic ramp proximal to the developing Taconic orogen: Lourdes  
706 Formation, Newfoundland, Canada. *Facies* 54, 121–149.
- 707 Benedetto, J.L., 1993. La hipótesis de la aloctonía de la Precordillera Argentina: un test  
708 estratigráfico y biogeográfico. 12° Congreso Geológico Argentino Actas 3, pp. 375-384.
- 709 Benedetto, J.L., Sánchez, T.M., Carrera, M.G., Brussa, E.D., Salas, M.J., 1999.  
710 Paleontological constraints in successive paleogeographic positions of Precordillera  
711 terrane during the Early Paleozoic. In: *Laurentia-Gondwana connections before Pangea*  
712 (eds. VA., Ramos & J.D., Keppie), pp. 21-42, Geological Society of America,  
713 Colorado. Special Paper 336.
- 714 Beresi, M.S., 1986. Paleoecología y biofacies de la Formación San Juan al sur del  
715 paralelo de 30° sur, Precordillera de San Juan. Tesis Doctoral en Ciencias Geológicas,  
716 Universidad Nacional de San Juan, pp. 1-400. Ph.D thesis.

- 717 Beresi, M.S., Rigby, J.K., 1993. The Lower Ordovician Sponges of San Juan,  
718 Argentina. *Brigham Young University Geology Studies* 39, 1-63.
- 719 Brett, C. E., Boucot, A. J., Jones, B. 1993. Absolute depths of Silurian benthic  
720 assemblages. *Lethaia* 26, 25-40.
- 721 Brett, C.E., Malgieri, T.J., Thomka, J.R., Aucoin, C.D., Dattilo, B.F., Schwalbach, C.E.,  
722 2015. Calibrating water depths of Ordovician communities: lithological and ecological  
723 controls on depositional gradients in Upper Ordovician strata of southern Ohio and  
724 north-central Kentucky, USA. *Estonian Journal of Earth Sciences* 64, 19-23.
- 725 Cañas, F.L. 1999. Facies and sequences of the Late Cambrian - Early Ordovician  
726 carbonates of the Argentine Precordillera: a stratigraphic comparison with Laurentian  
727 platforms. In: *Laurentia-Gondwana connections before Pangea* (eds. VA., Ramos &  
728 J.D., Keppie), pp. 43-62, Geological Society of America, Colorado. Special Paper 336.
- 729 Cañas, F.L. 2002. Selected sections of Lower to Middle Ordovician carbonate  
730 sedimentation of the Argentine Precordillera: The La Silla and San Juan formations at  
731 Cerros La Silla and Niquivil. *Miscelánea* 8, 5-20. Tucumán.
- 732 Cañas, F.L., Carrera, M.G., 1993. Early Ordovician microbial-sponge-receptaculitid  
733 bioherms of the Precordillera, Western Argentina. *Facies* 29, 169-178.
- 734 Cañas, F., Carrera, M.G., 2003. Precordilleran Reefs. In: *Ordovician fossils of*  
735 *Argentina* (ed. J.L., Benedetto). Secretaría de Ciencia y Tecnología, Universidad  
736 Nacional de Córdoba, pp. 131-154.
- 737 Cañas, F.L., Keller, M. 1993. Arrecifes y montículos arrecifales en la Formación San  
738 Juan (Precordillera sanjuanina, Argentina): Los arrecifes más antiguos de Sudamérica.  
739 *Boletín Real Sociedad Española de Historia Natural (Sc. Geología)*, 88, 127-136.



- 740 Carrera, M.G. 1997. Análisis paleoecológico de la fauna de poríferos del Llanvirniano  
741 tardío de la Precordillera Argentina. *Ameghiniana* 34, 309-316.
- 742 Carrera, M.G., Cañas, F., 1996. Los biohermos de la Formación San Juan (Ordovícico  
743 temprano, Precordillera Argentina): paleoecología y comparaciones. *Revista Asociación*  
744 *Argentina de Sedimentología* 3: 85-104.
- 745 Carrera, M. G., Astini, R. A., Gomez, F. A. 2017. A lowermost Ordovician tabulate-like  
746 coralomorph from the Precordillera of western Argentina: a main component of a reef-  
747 framework consortium. *Journal of Paleontology*, 91: 73 - 85.
- 748 Chen, D.Z., Guo, Z.H., Jiang, M.S., Guo, C., Ding, Y., 2016. Dynamics of cyclic  
749 carbonate deposition and biotic recovery on platforms during the Famennian of Late  
750 Devonian in Guangxi, South China: Constraints from high-resolution cycle and  
751 sequence stratigraphy. *Palaeogeography, Palaeoclimatology and Palaeoecology* 448,  
752 245–265.
- 753 Church, S., 1974. Lower Ordovician patch reefs in western Utah. *Brigham Young Univ.*  
754 *Geology Studies* 21: 41-62.
- 755 Cocks, L., Torsvik, T.H., 2002. Earth geology from 500 to 400 million years ago: A  
756 faunal and palaeomagnetic review. *Journal of the Geological Society*, 159: 631–644.
- 757 Dubinina, S. V., Ryazantsev, A. V., 2008. Conodont stratigraphy and correlation of the  
758 Ordovician volcanogenic and volcanogenic sedimentary sequences in the South Urals.  
759 *Russian Journal of Earth Sciences*, 10: 1-31.
- 760 Dunham, R., 1962. Classification of carbonate rocks according to depositional texture.  
761 *American Association of Petroleum Geologist, Memoir* 1, 108-121.

- 762 Ethington, R.L., Clark, D.L., 1981. Lower and Middle Ordovician Conodonts from the  
763 Ibex Area Western Millard County, Utah. Brigham Young University Geology Studies  
764 28(2), 159 pp.
- 765 Flügel, E., 2010. Microfacies of Carbonate Rocks. Analysis, Interpretation and  
766 Application. Springer-Verlag, Berlin-Heidelberg, pp. 976.
- 767 Guo, C., Chen, D., Song, Y., Zhou, X., Ding, Y., Zhang, G. 2018. Depositional  
768 environments and cyclicity of the Early Ordovician carbonate ramp in the western  
769 Tarim Basin (NW China). *Journal of Asian Earth Sciences* 158, 29–48.
- 770 Hamon, Y., Merzeraud, G., 2008. Facies architecture and cyclicity in a mosaic  
771 carbonate platform: effects of fault-block tectonics (Lower Lias, Causses platform,  
772 south-east France). *Sedimentology* 55, 155–178.
- 773 Haq, B.U., Shutter, S.R., 2008. A chronology of Paleozoic sea-level changes. *Science*  
774 322, 64-68.
- 775 Heredia, S., Mestre, A., 2011. Middle Darriwilian Conodont Biostratigraphy in the  
776 Argentine Precordillera. In: *Ordovician of the World* (eds. J.C., Gutiérrez Marco, I.,  
777 Rábano & D., García Bellido), pp. 229–234, Cuadernos del Museo Geominero 14.
- 778 Heredia, S., Mestre, A., 2013. Advances in the middle Darriwilian conodont  
779 biostratigraphy of the Argentine Precordillera. In: *Conodont from the Andes* (eds. G.,  
780 Albanesi & G., Ortega), pp. 45 – 48. 3° International Conodont Symposium. Asociación  
781 Paleontológica Argentina, Publicación Especial 13, Buenos Aires.
- 782 Heredia, S., Mestre, A., 2017. Primer registro del conodonte darriwiliano *Lenodus*  
783 *antivariabilis* an en la Precordillera Central de San Juan, Argentina. In *Estratigrafía y*

- 784 Paleontología del Paleozoico Inferior de Argentina (eds. J.L., Benedetto, S. Heredia &  
785 G., Aceñolasa), pp. 38-42. XX Congreso Geológico Argentino, Tucumán.
- 786 Heredia, S., Beresi, M., Mestre, A., Rodríguez, M.C., 2009. El Ordovícico en la Sierra  
787 de La Higuera (Mendoza): conodontes y microfácies. Serie Correlación Geológica 24,  
788 65-76.
- 789 Heredia, S., Carlorosi, J., Mestre, A., Soria, T., 2013. Stratigraphical distribution of the  
790 Ordovician conodont *Erraticodon* Dzik in Argentina. Journal of South American Earth  
791 Sciences 45, 224- 234.
- 792 Heredia, S., Mestre, A., Kaufmann, C., 2017. The Darriwilian conodont biostratigraphy  
793 from the Argentine Precordillera. In: Progress on Conodont Investigation (eds. J.- C.,  
794 Liao & J.I., Valenzuela-Rios) pp. 65-69. 4° International Conodont Symposium.  
795 Cuadernos del Museo Geominero 22, Valencia.
- 796 Herrera, Z., Benedetto, J.L. 1991. Early Ordovician brachiopod fauna from the  
797 Precordillera Basin, western Argentina: biostratigraphy and paleobiostratigraphical  
798 affinities. In: Brachiopods Through Time (eds. D.L., Mackinnon, D.E., Lee & J.D.,  
799 Campbell) pp. 283-301. 2nd International Brachiopod Congress Proceedings, University  
800 of Otago, Balkema, Totterdam.
- 801 Holland, S.M., 1993. Sequence stratigraphy of a carbonate-clastic ramp: The  
802 Cincinnati Series (Upper Ordovician) in its type area. Geological Society of America  
803 Bulletin 105, 306-322.
- 804 Hong, J., Oh, J-R, Lee, J-H, Choh, S-J., Lee D-J., 2018. The earliest evolutionary link  
805 of metazoan bioconstruction: Laminar stromatoporoid–bryozoan reefs from the Middle  
806 Ordovician of Korea. Palaeogeography, Palaeoclimatology, Palaeoecology 492, 126-  
807 133.

- 808 Johnston, D.I., Barnes, C.R. 1999. Early and Middle Ordovician (Arenig) conodontes  
809 from St. Pauls Inlet and Martin Point, Cow Head Group, Western Newfoundland,  
810 Canada. *Biostratigraphy and paleoecology. Geologica et Palaeontologica* 33: 21-70.
- 811 Kaya, A., Friedman, G.M., 1997. Sedimentation and facies analysis of the *Girvanella*  
812 constituted oncolitic shoals and associated lithofacies in the Middle Ordovician.  
813 Antelope Valley Limestone, Central Nevada, USA. *Carbonates and Evaporites* 12, 134-  
814 156.
- 815 Keller, M., 1999. Argentine Precordillera: Sedimentary and Plate Tectonic History of a  
816 Laurentian Crustal Fragment in South America. *Geological Society of America Special*  
817 *Paper* 341, 1-131.
- 818 Keller, M., Bordonaro, O., 1993. Arrecifes de estromatopóridos en el Ordovícico  
819 Inferior del oeste Argentino y sus implicaciones paleogeográficas. *Revista Española de*  
820 *Paleontología* 8, 165-169.
- 821 Keller, M., Flügel, E., 1996. Early Ordovician reefs from Argentina: stromatoporoid vs.  
822 stromatolite origin. *Facies* 34, 177-192.
- 823 Keller, M., Cañas, F., Lehnert, O., Vaccari, N.E., 1994. The Upper Cambrian and  
824 Lower Ordovician of the Precordillera (Western Argentina): Some stratigraphic  
825 reconsiderations. *Newsletters in Stratigraphy*, 31: 115-132.
- 826 Lehnert, O., 1993. Bioestratigrafía de los conodontes arenigianos de la Formación San  
827 Juan en la localidad de Niquivil (Precordillera sanjuanina, Argentina) y su correlación  
828 intercontinental. *Revista Española de Paleontología* 8 (2): 153-164.

- 829 Lehnert, O., 1995. Ordovizische Conodonten aus der Präkordillere Westargentiniens:  
830 Ihre Bedeutung für Stratigraphie und Paläogeografie. Erlangen geologische  
831 Abhandlungen, Erlangen, 125: 193 pp.
- 832 Lehnert, O., Keller, M., 1993. Posición estratigráfica de los arrecifes arenigianos en la  
833 Precordillera Argentina. Docum. Lab. Geól. Lyon, 125: 263-275.
- 834 Lehnert, O., Keller, M., Bordonaro, O., 1998. Early Ordovician conodonts from the  
835 southern Cuyania Terrane (Mendoza Province, Argentina). In: Proceedings of the Sixth  
836 European Conodont Symposium ECOS VI (ed. H. Szaniawski), pp. 47-65,  
837 Palaeontologica Polonica, v. 58.
- 838 Lehnert, O., Stouge, S., Brandl, P.A., 2013. Conodont biostratigraphy in the Early to  
839 Middle Ordovician strata of the Oslobreen Group in Ny Friesland, Svalbard. Zeitschrift  
840 der Deutschen Gesellschaft für Geowissenschaften, 164: 149–172.
- 841 Li, Q.J., Li, Y., Wang, J.P., Kiessling, W., 2015. Early Ordovician lithistid sponge–  
842 Calathium reefs on the Yangtze Platform and their paleoceanographic implications.  
843 Palaeogeography, Palaeoclimatology, Palaeoecology 425, 84–96.
- 844 Li, Q.J., Li, Y., Zhang, Y., Munnecke, A., 2017. Dissecting *Calathium*-microbial  
845 frameworks: The significance of calathids for the Middle Ordovician reefs in the Tarim  
846 Basin, northwestern China. Palaeogeography, Palaeoclimatology, Palaeoecology, 474,  
847 66-78.
- 848 Li, Q-J, Sone, M., Lehnert, O., Na, L., 2018. Early Ordovician sponge-bearing  
849 microbialites from Peninsular Malaysia: The initial rise of metazoans in reefs.  
850 Palaeoworld, <https://doi.org/10.1016/j.palwor.2018.08.005>.
- 851 Li, Z., Stouge, S., Chen, X., Wang, C., Wang, X., Zeng, Q., 2010. Precisely  
852 compartmentalized and correlated Lower Ordovician *Oepikodus evae* zone of the Floian

- 853 in the Huanghuachang section, Yichang, Hubei province. *Acta Palaeontologica Sínica*  
854 49, 108–124 (in Chinese with English abstract).
- 855 Lindskog, A., Eriksson, M. E., Tell, C., Terfelt, F., Martin, E., Ahlberg, P., Schmitz, B.,  
856 Marone, F., 2015. Mollusk maxima and marine events in the Middle Ordovician of  
857 Baltoscandia. *Palaeogeography, Palaeoclimatology, Palaeoecology*, 440, 53–65.
- 858 Löfgren, A., Zhang, J., 2003. Element association and morphology in some Middle  
859 Ordovician platform–equipped conodonts. *Journal of Paleontology* 77, 723–739.
- 860 Mángano, M.G., Droser, M., 2004. The ichnologic record of the Ordovician radiation.  
861 In: *The Great Ordovician Biodiversification Event* (eds. B., Webby, M., Droser, F.,  
862 Paris & I., Percival), pp. 369-379. Columbia University Press, New York.
- 863 Mango, M.J., Albanesi, G.L., 2018a. Conodont biostratigraphy from the upper San Juan  
864 Formation (Middle Ordovician) at Niquivil, Argentine Precordillera. *Journal of South*  
865 *American Earth Sciences* 84, 48-55.
- 866 Mango, M.J., Albanesi G.L., 2018b. Bioestratigrafía y provincialismo de conodontes  
867 del tramo medio-superior de la Formación San Juan en el cerro Viejo de Huaco,  
868 Precordillera, Argentina. *Andean Geology* 45 (2): 274-299.
- 869 Mestre, A., 2012. Bioestratigrafía de conodontes del techo de la Formación San Juan y  
870 el miembro inferior de la Formación Los Azules, Cerro La Chilca, Precordillera Central.  
871 *Ameghiniana* 49, 185-197.
- 872 Mestre, A., 2014. Bioestratigrafía de conodontos del Darriwiliense medio (Ordovícico)  
873 en el borde oriental de la Sierra de Villicum (Precordillera Oriental, Argentina). *Boletín*  
874 *Geológico y Minero* 125, 65-76.

- 875 Mestre, A., Heredia, S., 2013. Biostratigraphic significance of Darriwilian conodonts  
876 from Sierra de La Trampa (Central Precordillera, San Juan, Argentina). *Geosciences*  
877 *Journal* 17, 43 – 53.
- 878 Nielsen, A.T., 2003. Ordovician sea-level changes: potencial for global event  
879 stratigraphy. In: *Ordovician from the Andes* (eds. G., Albanesi, M., Beresi & S.,  
880 Peralta), pp. 445-449, Serie Correlación Geológica 17, Tucumán.
- 881 Nielsen, A.T. 2011. A re-calibrated revised sea-level curve for the Ordovician of  
882 Baltoscandia. In: *Ordovician of the World* (eds. J.C., Gutiérrez-Marco, I. Rábano & D.,  
883 García-Bellido) pp. 399-402, Instituto Geológico y Minero de España, Madrid.
- 884 Nitecki, M.H., 1972. North American Silurian Receptaculitid Algae, *Fieldiana Geology*  
885 28. Field Museum of Natural History, Chicago, pp. 108.
- 886 Pohler, S.M.L., James, N.P., 1989. Reconstruction of a Lower/Middle Ordovician  
887 Carbonate shelf margin: Cow Head Group, Western Newfoundland. *Facies* 21, pp. 189-  
888 262.
- 889 Pratt, B., James, N., 1982. Cryptoalgal-metazoan bioherms of early Ordovician age in  
890 the St. George Group, western Newfoundland. *Sedimentology* 29, 543-569.
- 891 Pratt, B., James, N., 1989. Coral-*Renalcis*-Thrombolite Reef Complex of Early  
892 Ordovician Age, St. George Group, Western Newfoundland. In: *Reefs, Canada and*  
893 *adjacent areas* (eds. H.J., Geldsetzer, N.P., James & G.E., Tebbutt) pp. 224-230,  
894 Canadian Society of Petroleum Geologists, Memoir 13.
- 895 Read, J.F., 1985. Carbonate platform facies models. *Bulletin of American Association of*  
896 *Petroleum Geologists* 69, pp. 1-21.

- 897 Riding, R., 1991. Classification of microbial carbonates. In: *Calcareous Algae and*  
898 *Stromatolites* (ed. R., Riding,) pp. 21– 51, Springer-Verlag, Berlin.
- 899 Riding, R. 2000. Microbial carbonates: the geological record of calcified bacterial–  
900 algal mats and biofilms. *Sedimentology* 47(Supplement 1), 179–214.
- 901 Riding, R. 2002. Structure and composition of organic reefs and carbonate mud mounds:  
902 concepts and categories. *Earth-Science Reviews* 58, 163–231.
- 903 Ross, R.J., Hintze, L.F., Ethington, R.L., Miller, J.F., Taylor, M.E., Repetski, J.E.,  
904 Sprinkle, J., Guensburg, T.E., 1997. The Ibexian, Lowermost Series in the North  
905 American Ordovician. U.S. Geological Survey, Professional Paper, 1579, 1–50.
- 906 Sánchez, T.M, Carrera, M.G., Benedetto, J.L., 1996. Variaciones faunísticas en el techo  
907 de la Formación San Juan (Ordovícico temprano, Precordillera Argentina): significado  
908 paleoambiental. *Ameghiniana* 33, 185–200.
- 909 Sarmiento, G., 1990. Conodontos ordovícicos de Argentina. *Treballs del Museu de*  
910 *Geología*, Barcelona 1, 135-161.
- 911 Soria, T., 2017. La Zona de *Oepikodus intermedius* (Ordovícico Inferior) en la  
912 Quebrada Los Sapitos, Precordillera Central, San Juan. In: *Estratigrafía y Paleontología*  
913 *del Paleozoico Inferior de Argentina* (eds. J.L, Benedetto, S., Heredia, G., Aceñolaza &  
914 J., Carlosi) pp. 32-37, XX Congreso Geológico Argentino, Tucumán.
- 915 Soria, T., Heredia, S., Mestre, A., Rodríguez, C., 2013. Conodontes floianos de la  
916 Formación San Juan en la quebrada de Talacasto, Precordillera de San Juan. *Serie de*  
917 *Correlación Geológica* 29, 93-106.
- 918 Soria, T., Mestre, A., Morfil, A., Benegas, L., Heredia, S., 2017. Bioestratigrafía de  
919 conodontes de los biohermos de estromatoporoides de la Formación San Juan en  
920 Niquivil y Talacasto, Precordillera Central. In: *Estratigrafía y Paleontología del*



- 921 Paleozoico Inferior de Argentina (eds. J.L. Benedetto, S., Heredia, G., Aceñolaza & J.,  
922 Carlorosi) pp. 87-91, XX Congreso Geológico Argentino, Tucumán.
- 923 Stearn, C. W., Webby, B. D., Nestor, H., Stock, C. W., 1999. Revised classification and  
924 terminology of Palaeozoic stromatoporoids. *Acta Palaeontologica Polonica* 44 (1): 1–  
925 70.
- 926 Stone, J., 1987. Review of investigative techniques used in the study of conodonts. In:  
927 *Conodonts: Investigative Techniques and Applications* (ed. R., Austin), pp. 17-34, Ellis  
928 Horwood Limited, Chichester.
- 929 Thomas, W.A., Astini, R.A., 1996. The Argentine Precordillera: A traveler from the  
930 Ouachita embayment of North American Laurentia. *Science* 273, 752-757.
- 931 Thomas, W.A., Tucker, R.D., Astini, R.A. 2000. Rifting of the Argentine Precordillera  
932 from southern Laurentia: palimpsest restoration of basement provinces. *Geological*  
933 *Society of America, Abstracts with Programs* 32, pp. A-505.
- 934 Toomey, D.F., 1970. An unhurried look at a Lower Ordovician mound horizon,  
935 Southern Franklin Mountains, West Texas. *Journal of Sedimentary Petrology* 40, pp.  
936 1318-1334.
- 937 Toomey, D.F., Babcock, J.A., 1983. Precambrian and Paleozoic algal carbonates, west  
938 Texas-southern New Mexico. *Professional Contributions Colorado School of Mines* 11,  
939 1-345.
- 940 Toomey, D.F., Ham, W.E. 1967. *Pulchrilamina*, a new mound-building organism from  
941 Lower Ordovician rocks of West Texas and South Oklahoma. *Journal of Paleontology*  
942 41, 981-987.

- 943 Toomey, D.F., Nitecki, M., 1979. Organic build-ups in the Lower Ordovician  
944 (Canadian) of Texas and Oklahoma. *Fieldiana* 2, pp. 181.
- 945 Vaccari, N.E., 1994. Las faunas de trilobites de las sucesiones carbonáticas del  
946 Cámbrico y Ordovícico temprano de la Precordillera Septentrional Argentina. Tesis  
947 Doctoral en Ciencias Geológicas, Facultad de Ciencias Exactas, Físicas y Naturales.  
948 Universidad Nacional de Córdoba, pp. 1- 271. Ph. D. thesis.
- 949 Viira, V., Löfgren, A., Mägi, S., Wickström, J., 2001. An Early to Middle Ordovician  
950 succession of conodont faunas at Mäekalda, northern Estonia. *Geological Magazine*,  
951 138, 699-718.
- 952 Wang, X.F., Stouge, S., Chen, X.H., Li, Z.H., Wang, C.S., Finney, S.C., Zeng, Q.L.,  
953 Zhou, Z.Q., Chen, H.M., Zhang, M., Xu, G.H., Erdtmann, B.-D., 2009. The Global  
954 Stratotype Section and Point for the Middle Ordovician Series and the Third Stage  
955 (Dapingian). *Episodes* 32 (2), 96–114.
- 956  
957 Wang, Z-H, Zhen, Y-Y, Bergström, S., Wu, R-Ch., Zhang, Y-D., Ma, X., 2018. A new  
958 conodont biozone classification of the Ordovician System in South China. *Palaeoworld*.  
959 <https://doi.org/10.1016/j.palwor.2018.09.002>.
- 960 Webby, B. D., 1986. Early stromatoporoids. In: *Problematic Fossil Taxa* (Eds. A.,  
961 Hoffman & M. H. Nitecki), pp. 148–166, Oxford Monograph on Geology and  
962 Geophysics 5.
- 963 Webby, B. D., 2002. Patterns of Ordovician reef development. In: *Phanerozoic Reef*  
964 *Patterns* (eds. W., Kiessling, E., Flügel & J., Golonka,), pp. 129-179, SEPM Special  
965 Publication 72, Tulsa.
- 966 Webby, B. D., 2012. Part E, Revised, Volume 4, Chapter 17: Class Uncertain, Order  
967 Pulchrilaminida, new order. *Treatise Online* 30, pp. 1–9.

- 968 Zhang, Y.Y., Li, Q., Li, Y., Kiessling, W., Wang, J.P., 2016. Cambrian to Lower  
969 Ordovician reefs on the Yangtze Platform, South China Block, and their controlling  
970 factors. *Facies* 62, 17, doi.10.1007/s10347-016-0466-8.
- 971 Zhang, Y.Y., Wang, J.P., Li, Y., 2015a. Bank facies from the Upper Ordovician  
972 Lianglitag Formation in the Central Tarim Oil Field, NW China. *Acta*  
973 *Micropalaeontologica Sinica* 32, 95-104 (in Chinese with English abstract).
- 974 Zhang, Y.Y., Wang, J.P., Munnecke, A., Li, Y., 2015b. Ramp morphology controlling  
975 the facies differentiation of a Late Ordovician reef complex at Bachu, Tarim Block, NW  
976 China. *Lethaia* 48, 509–521.
- 977 Zhen, Y.Y., Pickett, J.W., 2008. Ordovician (Early Darriwilian) conodonts and sponges  
978 from west of Parkes, central New South Wales. *Proceedings of the Linnean Society of*  
979 *New South Wales* 129, 57-82.
- 980 Zhen, Y-Y., Nicoll, R. S., Percival, I., Hamedi, M. A., Stewart, I., 2001. Ordovician  
981 rhipidognathid conodonts from Australia and Iran. *Journal of Paleontology*, 75(1),186-  
982 207.
- 983 Zhu Z., Liu, B. & Li, X., 1993. *Pulchrilamina* found in Early Ordovician reef at  
984 Huanghuachang, Yichang, Hubei. *Oil and Gas Geology* 14, 304–309. (In Chinese with  
985 English abstract).
- 986
- 987
- 988
- 989
- 990

991 **Table 1:** Conodont distribution in the Niquivil and Talacasto sections.

	Niquivil section						Talacasto section				
	J	K	L	M	P	S	T8	T9	T15b	T18	T20
<i>Ansella jemtlandica</i>											X
<i>Berg. extensus</i>	X	X	X	X	X		X	X		X	
<i>Cooperig. aranda</i>							X	X	X	X	
<i>Cornuodus longibasis</i>	X	X					X	X			
<i>Drepanodus arcuatus</i>	X	X			X		X	X			
<i>Drepanoistodus forceps</i>	X										
<i>Erraticodon patu</i>									X		
<i>Juanognathus jaanussoni</i>						X			X		X
<i>Juanognathus variabilis</i>	X				X		X	X		X	X
<i>Oepikodus evae</i>							X				
<i>Oepikodus intermedius</i>	X				X		X	X			
<i>Oistodus striolatus</i>			X	X		X	X	X	X		X
<i>Paroistodus parallelus</i>		X					X	X		X	
<i>Periodon flabellum</i>	X				X		X	X	X		
<i>Protop. leonardii</i>	X	X	X		X		X	X	X		
<i>Reutterodus andinus</i>							X				
<i>Rossodus barnesi</i>	X						X	X		X	X
<i>Scolopodus krummi</i>			X				X	X		X	
<i>Semiac. potrerillensis</i>			X			X					X
<i>Triangulodus sp.</i>						X			X	X	

993 **Table 2:** Carbonate facies and microfacies of the shoal and reef facies from the San  
 994 Juan Formation.

Facies and Microfacies		Lithology	Components	Siliciclastics	Texture and geometry	Interpretation
Facies 1	M1- Nodular Biointraclastic wackestone-packstone	Light to medium grey, fine skeletal wackestone-packstone, diverse and abundant robust fauna, little evidence of fossil erosion.	Gastropods (up to 80 %), intraclasts, minor brachiopods, <i>Halysis monoliformis</i> , <i>Nuia sibirica</i> , trilobites, and pelmatozoan ossicles. Rare peloids	Thin interbeds of silty shale	Dominantly thinly bedded; irregular to nodular. Shales occur as thin discontinuous laminae or burrow fill.	Shallow subtidal below wave action, occasionally storm reworked deposit.
	M2- Biointraclastic packstone-grainstone	Light to medium grey, fine to very coarse grainstone, well sorted	<i>Nuia sibirica</i> , <i>Halysis monoliformis</i> , pelmatozoan ossicles, oncoids, cortoids, intraclasts, peloids, trilobites, brachiopods, nautiloids, gastropods and ostracods	Silt to fine sands are rare to scarce, quartz	Coarse and tabular bedded with sharp erosive bases, massive and occasionally cross-bedding.	Moderate to high energy shoals bank, highly winnowed.
	M3-Microbialite-skeletal boundstone	Light grey, peloidal micrite	Microbial ( <i>Girvanella</i> sp., <i>Renalcis?</i> sp, among others), <i>Zondarella communis</i> , Sponges, <i>Calathium</i> sp., brachiopods, trilobites, pelmatozoan ossicles. peloids	Absent	Irregular to nodular, lateral discontinuous beds, domical to bell shapes	Reefs matrix supported, shallow subtidal in the shoal (M2), moderate energy.

<b>Facies 3</b>	<b>M4- Intra-bioclasic grainstone</b>	Light to reddish grey, medium to very coarse grained grainstone, diagenetic chert and iron oxide staining bioclasts	Pelmatozoan ossicles and articulate stems, <i>Girvanella</i> sp., oncoids intraclasts, fragmented <i>Calathium</i> sp., sponges, brachiopods, bryozoans, bioclastic fragments, peloids	Fine to very coarse quartz and lithic clasts	Thin to very thick tabular beds, thickest beds are continuous; erosive base and sharp top, amalgamated and stacked beds	High to moderate energy, shoal banks, shallowing-up cycles, hardground development
	<b>M5- Peloidal packstone-grainstone</b>	Light grey fine grainstone to packstone  diagenetic chert and nodules iron oxide	Peloids, pelmatozoan ossicles, sponges, brachiopods, gastropods and trilobites	Fine to very coarse quartz and lithic clasts	Thin to medium tabular beds, sharp, erosive bases. Burrowed tops; planar lamination, low-angle cross-stratification, locally amalgamated	

995

996

**New insights on Lower Ordovician (Floian) reefs from the Argentine Precordillera: biostratigraphic, sedimentologic and paleogeographic implications**

- The shallow facies of the middle part from the San Juan Formation were studied.
- Reef and shoal facies were recorded for the first time at the Talacasto section.
- Reef framework consists of calcimicrobes, pulchrilaminids, calathids and sponges.
- *Oepikodus intermedius* conodont Zone (Early Ordovician) was recorded.
- The pulchrilaminid *Z. communis* is assigned for first time to the late Floian.

16 May 2020

Dear Editor of the Journal of South American Earth Sciences:

We declare that we have no conflict of interest.

Journal Pre-proof